PHYSICAL REVIEW D **89,** 094001 (2014)

New regimes of the stringy (holographic) Pomeron and high-multiplicity *pp* and *pA* collisions

Edward Shuryak and Ismail Zahed

Department of Physics and Astronomy, Stony Brook University, Stony Brook, New York 11794, USA
(Received 10 February 2014; published 2 May 2014)

Holographic AdS/QCD models of the Pomeron unite a string-based description of hadronic reactions of the pre-QCD era with the perturbative BFKL approach. The specific version we will use due to Stoffers and Zahed [1–5], is based on a semiclassical quantization of a "tube" (closed string exchange or open string virtual pair production) in its Euclidean formulation using the scalar Polyakov action. This model has a number of phenomenologically successful results. The periodicity of a coordinate around the tube allows the introduction of a Matsubara time and therefore an effective temperature $T_{\rm eff}$ on the string. We observe that at the LHC energies and for sufficiently small impact parameter, $T_{\rm eff}$ approaches and even exceeds the Hagedorn temperature of the QCD strings. Based on studies of the stringy thermodynamics of pure gauge theories we suggest that there should exist two new regimes of the Pomeron: the "near-critical" and the "postcritical" ones. In the former one, string excitations create a high-entropy "string ball," with high energy and entropy but small pressure and free energy. If heavy enough, this ball becomes a (dual) black hole. As the intrinsic temperature of the string exceeds the Hagedorn temperature, the ball becomes a postcritical explosive "QGP ball." The hydrodynamical explosion resulting from this scenario was predicted [6] to have radial flow exceeding any ever seen, even in heavy ion collisions, which was recently confirmed by CMS and ALICE at LHC. We also discuss the elastic scattering profile, finding some hints for new phases in it, as well as two-particle correlations.

DOI: 10.1103/PhysRevD.89.094001 PACS numbers: 12.38.Aw, 11.25.Tq, 12.38.Mh

I. INTRODUCTION

A. The main ideas

Historically, the description of strong interactions has been shifting between an emphasis on perturbative and nonperturbative physics. This can be seen in the theory of hadronic collisions as well. The phenomenology of the 1960 s and 1970 s has revealed Pomeron and Reggeon exchanges, which later—due to Veneziano and others—were shown to be related with strings. The discovery of QCD gave rise to weak coupling approaches, instrumental for hard processes. When theorists turned to hadronic collisions in the Regge kinematic $s \gg |t|$ in the perturbative approach, they found the so-called BFKL Pomeron [7], through the resummation of gluonic ladders. These two roads to the Pomeron created some confusion, some authors even assumed there are two distinct objects in the scattering amplitude. This however contradicts phenomenology: there is a single amplitude with two different limits. Let us compare with a simpler and more familiar problem, static potential between two color charges. It too has a stringy behavior $V \sim r$ at large distances and a Coulombic one $V \sim 1/r$ at small distances.

After the discovery of the AdS/CFT correspondence, it became clear that one can have a unifying description for both regimes. Strings in holographic AdS_5 space with conformal properties produce Coulombic potential, and if this space has some "confining wall" at its IR, they obtain the confining regime as well. In this work we will use a particular version of such a model with a wall, applied to Pomeron by Stoffers, Zahed and others [1–3,5] and based on scalar Polyakov strings propagating in the five-dimensional holographic space. A historical evolution of the pomeron in holography can be found in a number of references within the past decade [8–14].

(Such holographic models, while conformal at small distances, are still not QCD-like, remaining strongly coupled. In the last decade development of a new generation of holographic models, collectively called AdS/QCD, try to unify weak and strong coupling regimes within the same framework by using dilaton field with tuned potential to mimic weak coupling and large momentum transfer $|t| \gg \Lambda^2_{\rm QCD}$. We are not using such models in this work, but may do so elsewhere.)

The understanding of the dynamics behind Pomerons and Reggeons still remains a challenging task. Traditionally models have been judged by their predictions on a rather limited number of observables, such as the dependence of the total and elastic cross sections on s and diffraction, related with certain fluctuations in the system. A new turn of events has taken place at the beginning of the LHC operation which has allowed to trigger on very high multiplicity events [15–19]. These events bring about novel issues related to strong fluctuations in the collision system.

Before we delve into the specifics of our analysis, let us identify our main idea. In the macroscopic (thermodynamical) context it is well known that the perturbative quark-gluon phase and the nonperturbative confining (stringy) phase are related by a first order phase transition (for

 © 2014 American Physical Society

$N_c > 2$ which we imply here). We argue that the same should be true for high energy scattering, as a function of the impact parameter, with all three regimes present in the scattering amplitude.

It is a well known fact, that explaining confinement starting from gluons is an extremely difficult (not yet completed) task. On the other hand, going in the opposite direction—from strings into the perturbative phase—is easier, and it was in fact qualitatively understood long ago. In the stringy approach an explanation is in terms of the so-called Hagedorn phenomenon [20]. Strings have exponentially rising density of states, as first noted by Fubini and Veneziano [21]. The explicit expression for the density of states $d(n)$ appeared in Huang and Weinberg [22], with cosmological consequences a la Hagedorn. A decade later, after the discovery of QCD and its formulation on the lattice, this fact re-surfaced again in finite-temperature QCD, through the work of Polyakov and Susskind [23,24].

Based on the analogy to thermodynamics of the glue (for some technical details and references see Sec. III) we will argue that in high energy collisions the excitations of the exchanged nonperturbative objects (two open strings or a closed string) should also proceed subsequently through three distinct stages, as one proceeds from more peripheral to more central collisions:

(1) A "cold" or subcritical regime, with low string excitations, that generates a Pomeron with a Gaussian profile.
(2) A "near-critical" regime, in which the exchanged string effectively decreases its tension due to the Hagedorn phenomenon, but increases its energy and entropy and turns to a "string ball." With the inclusion of self-interaction, the excited string is prone to implosion. It reduces its size and transmutes to a black hole. The corresponding transitory object is called a string hole (SH).
(3) A supercritical or "explosive" regime, in which the string becomes a black hole (BH), corresponding effectively to string breaking and the deconfined QGP phase. The Hawking radiation creates a perturbative thermal state, which generates sufficient pressure and leads to hydrodynamical explosion.

A sketch of the scattering amplitude versus the (squared) impact parameter $\mathbf{b}^2$, displaying all three regimes, is shown in Fig. 1. The details of the plot as well as the approximations used and the objects under considerations will be clarified as we proceed. At this point, let us just supply a sketch of the string ball, in Fig. 2. If heavy enough, its (effective) gravity may generate an effective trapped surface, shown by a gray circle. While we do not investigate the existence and properties of the trapped surfaces in this work, we would like to mention two works [25,26] which did study those, in different but related context, and concluded that the trapped surface suddenly disappears above a critical value of the impact parameter.

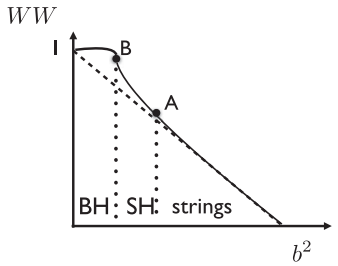

FIG. 1. Schematic representation of the log of the dipole-dipole scattering amplitude as a function of the squared impact parameter $\mathbf{b}^2$. The dashed line is the Gaussian-shaped string amplitude. The solid line represents the result, in three different regimes. For an explanation of BH (black hole) and SH (string hole), see text.

Returning to recent developments, we note that the current LHC experiments provide high luminosity and high-rate detectors, capable to detect and study very low probability fluctuations of the system. In the first LHC pp run, the CMS collaboration [15] has used this opportunity and triggered on events with high multiplicity. This was followed by similar (but much less expensive) triggered studies in pPb [16]. Multiple studies to follow—including experimental [17–19] and theoretical papers associated those observations with the production of a small-size hot fireball made of a Quark-Gluon Plasma (QGP), that explodes hydrodynamically. Those recent papers include ours [6], in which we predicted that the radial flow in high multiplicity pp and pA events should be even stronger than in AA collisions. Radial flow has been recently observed by CMS and ALICE via spectra of identified particles, confirming our theoretical prediction.

The paper is structured as follows: Since we aim at rather different readers, from heavy ion experimentalists to string theorists, we provide two more subsections of the Introduction containing a brief introduction to the Pomeron phenomenology and its stringy description I B, as well as the thermodynamics of the glue I D. (Experts obviously may omit some of that.) The main body of the paper starts in Sec. II from a review of glueball Regge trajectories I C

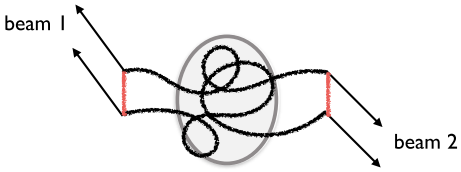

FIG. 2 (color online). A sketch of a string configuration at $t = 0$, as it appears from the under-the-barrier Euclidean domain. The small size dipoles are an approximation to colliding protons. At $t = 0$ they are separated by the transverse distance $\mathbf{b}$, the impact parameter. They move in the direction shown by two arrows later. The gray shaded sphere indicates a gravitational trapped surface.

and their relation to particle correlations. We emphasize the role of correlation measurements for finding "clustering" of hadrons, related in the Regge language with the exchange of the excited ("daughter") Pomerons. In Sec. II A we introduce the physical setting and the main results of the SZ Pomeron model, including its weak coupling limit II B and daughter trajectories II C.

The core of the paper is Sec. III devoted to quantum fluctuations of the exchanged strings. In spite of the fact that we are dealing with a zero temperature scattering amplitude, in subsection III A we explain that string excitations naturally have a thermodynamical description including temperature and entropy. Those take the central stage as we discuss in Sec. IV the near-critical regime and in Sec. V the supercritical one. The main ideas happen to be well developed in the string theory literature. They include the transition to a black hole and a "thermal scalar formalism." Section VI discusses observable consequences of the scenario. Subsection VI A is devoted to the elastic scattering amplitude. We compare our predictions with a parametrization of the data, and show that it contains evidences of the change of behavior consistent with our interpretation. In subsection VI B we discuss predictions for a cluster produced in high multiplicity inelastic collision, in particular its t-channel description in terms of the Pomeron daughter exchange. The remainder of the paper contains additional theoretical considerations, further elucidating the connection between a string ball and a black hole, see Sec. VII B. One result is the value of the "string viscosity", and also a discussion of the Hawking radiation VII C. In our final discussion section we provide a summary of the results VIII A.

B. Pomerons, Reggeons and QCD strings

The Pomeron is an effective object corresponding to the highest Regge trajectory $\alpha(t)$ and dominating the high energy cross sections at small $|t| \ll s$

$$\frac{d\sigma}{dt} \approx \left(\frac{s}{s_0}\right)^{\alpha(t)-1} \approx e^{\ln(s)(\alpha(0)-1)+\alpha' t} \tag{1}$$

Dimensionless $\alpha(0)$ is called the intercept of the Regge trajectory $\alpha(t)$, it explains the energy dependence of the cross sections. The first derivative $\alpha'(0)$ describes the spatial size of the Pomeron: it is related to the string tension, and is used ever since as the basic string scale, both in QCD and fundamental string theory. Unitarity relates total cross section to imaginary part of the forward elastic amplitude, which is thus the main objects to be discussed below. Regge trajectories, including the Pomeron, have physical states at positive t and integer $J = \alpha(t)$, see below.

Originally Pomeranchuk and Gribov [27] suggested a universal pole with vacuum quantum numbers and the intercept $\alpha_P(0) - 1 = 0$, corresponding to an asymptotically constant cross sections. The discovery of slowly rising cross sections $\sigma_{hh}(s)$ led to the so-called "supercritical soft Pomeron" with $\alpha_P(0) - 1 \approx 0.08$. Regge trajectories with various quantum numbers are subdominant and the corresponding cross sections are decreasing powers of s. For example the leading ρ meson trajectory has $\alpha_\rho(0) - 1 \approx -0.5$. The glueball (Pomeron daughters) excitations have even smaller intercepts $\alpha_{P_n}(0) < 0$ to be discussed below.

Diffractive processes with large rapidity gaps were described in terms of interacting Pomerons and Reggeons, which led Gribov [28] and others to formulate some effective Reggeon Field Theory. Important for the applications to diffractive and inelastic processes are the so-called AGK cutting rules [29]. At large $\sqrt{s}$ it is a nonrelativisticlike field theory of interacting particles (wee partons) diffusing in transverse dimensions, with the rapidity playing the role of time. The concept of Gribov diffusion explains why the transverse size of a hadron grows with $\ln(s/s_0)$ (the rapidity or "time" interval), as observed in pp and $p\bar{p}$ scattering. Pomerons interact but with a small triple-Pomeron vertex. For recent Pomeron parameters and a fit to the LHC data on cross sections and multiplicities see e.g. [30]. We note that the intercept for the "input Pomeron" used there is $\alpha_{\mathbf{P}}(0) - 1 \approx 0.25$, amusingly similar to our starting Pomeron in flat space.

In the pre-QCD period, the discovery of many s-channel resonances with conjectured t-channel Reggeon exchanges led Veneziano to the famed amplitude for the scattering of two scalars possessing planar duality between the s- and t-channel poles [31]. This observation, was soon generalized to the scattering of N scalars and the dual resonance model. The various attempts to understand the meaning of these formulas led to the idea of quantum strings rather than particles, underlying the string interactions at strong coupling. (This in turn led to the discussion about the internal consistency of the string formulation and to the fundamental superstring theory.)

Gribov partonic description of the Pomeron and its transverse diffusion follows from QCD at weak coupling by resumming rapidity ordered gluon or BFKL ladders [7]. At large $\sqrt{s}$ collinear gluon bremsstrahlung is large even at weak coupling and requires resummation. The one-loop BFKL resummed ladders lead to a perturbative Pomeron with a large intercept and zero slope. (A formidable two-loop calculation of the intercept of the QCD perturbative Pomeron raises, once again, the issue of convergence of the perturbative series at such t.)

The t'Hooft large N_c with $\lambda = g^2 N_c$ fixed, and its planar diagrammatics led to speculations that at strong coupling perturbative "fish-net" diagrams generate a surface [32]. The discovery of string-gravity duality in the AdS/CFT holographic context [33] makes the speculation more quantitative for certain gauge theories, unfortunately not (yet) for confined QCD.

A schematic picture of the (color) dipole-dipole scattering via a tubed-shaped surface exchange is shown in Fig. 3.

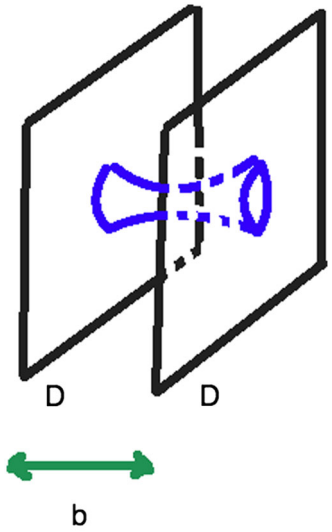

FIG. 3 (color online). Dipole-dipole scattering due to closed string exchange. The impact parameter **b** is the dipole transverse separation.

It can be alternatively viewed as an exchange of a closed string glueball state, or a virtual production of a pair of open strings, which later annihilate each other. The derivation of the elastic and inelastic amplitudes generated by surface exchanges were addressed using bosonic variational surfaces [8–10], see also a black-disk model [12].

(It has been realized that in pure AdS with $\mathcal{N}=4$ supersymmetry and conformal symmetry the dominant scattering mechanism should be associated with a spin-2 graviton exchange [11]. This is not the case in the setting we have. In particular, the main contribution is to the real part of the scattering amplitude, not related with inelastic events we discuss.)

To put things in perspective it is worth reviewing the phenomenology of the elastic pp cross section $d\sigma/dt$. Its behavior is studied experimentally all the way to LHC energies, see especially the results of the TOTEM collaboration at $\sqrt{s}=7$ TeV in [34]. In short there is a very accurate exponential $e^{\alpha' t}$ behavior at small $|t|$, for several decades, followed by a dip at $|t|=0.53$ GeV and then a power-like tail $|t|^{-p}$ with $p\approx 7.8$. A single dip means that the imaginary part of the amplitude changes sign once.

While experimentally elastic scattering is measured as a function of momentum transfer, for theoretical analysis it is convenient to use the impact parameter representation of the scattering amplitude, connected with the momentum transfer via a Bessel transform,

$$\mathcal{T}(s,q)=s\int_0^\infty d\mathbf{b}\mathbf{b}J_0(\mathbf{b}q)F(s,\mathbf{b}), \tag{2}$$

where $t=-q^2$. The so-called scattering profile $F(s,\mathbf{b})$ tells us about the "opacity" of scattered objects when their centers are separated by a particular impact parameter b. Like the static potential, one expects this profile to be string-dominated at large b and conformal-perturbative at small b. After this profile is calculated in some model, holographic or not, the scattering amplitude can be recovered by the inverse Bessel transform.

Since each set of data is taken only at some interval of t, their direct Bessel-transform to coordinate space always include extrapolations. Instead of doing it numerically with data, one can do it instead analytically, with available parametrizations. Being a function of two variables—s, t—it can be parametrized in multiple ways, and there is no shortage of models which can fit it. An example is the Bourrely-Soffer-Wu (BSW) model [35], see their expressions (13)–(15). These profiles are plotted in Fig. 4 for pp collisions, at LHC and ISR energies.

While the lower ISR energies have near-Gaussian shape, the LHC ones display three regions: (i) a nearly horizontal plateau, (ii) a relatively rapid turn downward, and (iii) an exponential tail [36]. In order to see the boundaries of such three region more clearly, we also plotted in the lower plot of Fig. 4 the second derivative of the profile function $F(s,\mathbf{b})$, at LHC energy. One can clearly see a positive and

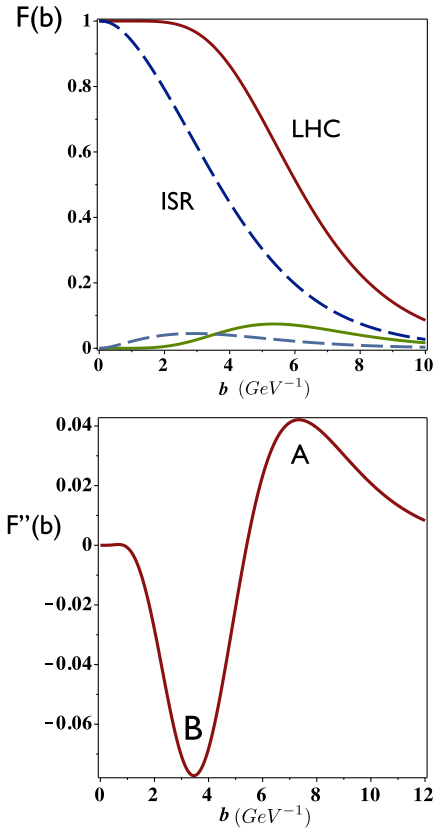

FIG. 4 (color online). The upper figure shows the imaginary (upper) and real (down) parts of the profile function $F(s,b)$ versus $\mathbf{b}(\mathrm{GeV}^{-1})$ for $\sqrt{s}=7$ TeV (solid) and $\sqrt{s}=63$ GeV (dashed). The lower plot shows the second derivative over b for $\sqrt{s}=7$ TeV. Two maxima correspond to the same points A, B as in the sketch in Fig. 1.

negative peak, indicating the "turning points" of the profile. We will argue below that these three regimes—as a function of **b**—correspond to the three dynamical regimes of a stringy Pomeron discussed in this work.

C. Glueball Regge trajectories

Nowhere in this paper the presence of quarks—as fundamental color charges—in QCD would be important, as all objects discussed are made of glue. Of course, quarks lead to string breaking (into mesons). However, this is a tunneling and rather suppressed phenomenon, happening later in the process, after the system is out of its initial Euclidean phase.

Therefore in this paper we completely abstract ourselves from the existence of quarks (and quark-related states, the corresponding Regge trajectories etc.) and discuss only the physical states of pure gauge theory, the glueballs. The glueball spectroscopy on the lattice is well developed, see e.g. [37,38], but it is not widely known, so we will briefly review it.

In Fig. 5 we display a compilation of all $J^{PC} = J^{++}$ states defined in the lattice simulations [38]. Before we come to our main issue—glueball Regge trajectories, a general comment is in order. The lowest states—which can be made of two gluons—are scalar 0^{++} and tensor 2^{++} ones. The forces mediated by those are both of attractive nature. (Those are in a way the "holographic images" of the bulk graviton and dilaton of AdS/QCD, which generate massive states in the presence of the wall.)

There are several Regge trajectories associated to these states. The upper one includes four states, the Pomeron and the $J^{++} = 2^{++}, 4^{++}, 6^{++}$ states. Its quadratic fit is

$$J = \alpha(0) + \alpha'(0)M^2 + \frac{\alpha''(0)}{2}M^4,$$
$$\alpha'(0) = 0.92/M_{2++}^2, \alpha''(0) = 0.05/M_{2++}^4, \quad (3)$$

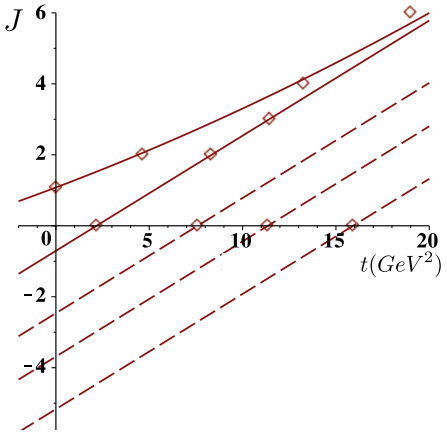

FIG. 5 (color online). Glueball Regge trajectories from lattice [38].

using units of $M_{2++} = 2.15$ GeV. Its continuation to negative $t = -M^2$ is separately observable in scattering experiments.

The "first daughter" trajectory, consisting of three states $J^{++} = 0^{++}, 2^{*++}, 3^{++}$, seems to be quite linear with a negative intercept. Using the "input Pomeron" [30] one finds the intercept gap,

$$\Delta\alpha_1 = \alpha_P(0) - \alpha_{D1}(0) \approx 2.0. \quad (4)$$

The next three daughter trajectories (also indicated on the plot by the dashed lines) have only one–the scalar–excited glueball in [38], so in the plot we had to assume that all daughters share the same slope (of course this needs not be generally correct). The second gap,

$$\Delta\alpha_2 = \alpha_P(0) - \alpha_{D2}(0) \approx 4, \quad (5)$$

which is in overall agreement with the holographic result (34) below, with the gaps 2 and 4, respectively.

The difference in slopes $\alpha'_{D1} > \alpha'_P$, observed in the glueball spectra is not predicted by the string models in flat space. Physically this difference means that the states of the daughter trajectories have larger spatial size than the Pomeron one. Since the second daughter trajectory corresponds to even higher excitations, their size and thus their slope α'_{D2} is perhaps also larger than α'_{D1}. Thus the gap between the intercepts $\Delta\alpha_2$ is perhaps larger than the estimate above.

As the number of states with momentum J is $J(J+1)$ and $M_J \sim \sqrt{J}$ one might think that the density of states grows as a power of the mass. However, this is not so. The number of stringy excitations grows with the mass exponentially. Thus, on one hand the states are on near-straight and approximately equidistant Regge trajectories. On the other hand, the number of states grows exponentially. The resolution of these seemingly contradicting statements lies in the fact that the daughter Regge trajectories must be multiply degenerate (which is not shown on the figure, of course, as only special quantum numbers are selected). The high degeneracy $d(n)$ of the daughter trajectories with $n > 0$ will be discussed in what follows.

D. QCD strings and thermodynamics of the glue

The most obvious and well known manifestation of the existence of the QCD strings is the approximate linear potential at large distances,

$$V(r) \approx \sigma_T r, \quad (6)$$

between fundamental color charges. Stringy excitations manifest themselves in corrections to the linear potential, starting with the famed Luscher term $\mathcal{O}(1/r)$ and its subleading corrections. Excitations of a string with particular quantum numbers have also been carried on the lattice. For a review discussing lattice results and their

effective stringy description at various N_c see [39]. In short, the lattice results indicate that the Nambu-Goto action—tension times the area of the string world volume—successfully describes all of those data.

Here, we mention an important theoretical result derived by Arvis [40], whereby the resummed potential induced by the fluctuations of the Nambu-Goto string resulted in the famous square root form,

$$V(r) = \sqrt{\frac{r^2}{(2\pi\alpha')^2} - \frac{D_\perp}{24\alpha'}}. \tag{7}$$

Its expansion generates the so-called universal Luscher terms mentioned above.

In absolute values the string tension

$$\sigma_T \approx (0.42\ \text{GeV})^2 \tag{8}$$

sets up the basic string units,

$$2\pi\sigma_T = \frac{1}{\alpha'} = \frac{1}{l_s^2}. \tag{9}$$

Furthermore, following lattice conventions, we will also use it to define "GeV" in all other confining theories, including $SU(N_c)$ gluodynamics.

Lattice simulations of gauge theories at finite temperatures and $N_c > 2$ display a first order transition $T_c \approx 0.27$ GeV. (For details, such as the N_c dependence of the critical temperature T_c and the latent heat see [39].) The thermodynamics of the glue at $T < T_c$ is very specific. Since the masses of the glueballs (discussed above) are numerically large compared to T, they make an extremely dilute gas. But the strings have so many states that the excitations happen to originate from the more massive states with an exponentially rising degeneracy.

As emphasized by Hagedorn [20], systems with exponentially growing density of states have very peculiar thermodynamics, e.g., the thermal partition sum,

$$Z(T) = \int dE e^{E/T_H} e^{-E/T}, \tag{10}$$

diverges as $T \to T_H$, known as the Hagedorn temperature. Historically, Hagedorn originally had a different picture of hadrons, as bags within bags in the bootstrap sense, not strings. Hagedorn originally concluded that there exists a fundamental upper bound on temperatures, as such systems can reach infinite energy density with $T \to T_H$. The emergence of QCD in the seventies and the development of the theory of the quark gluon plasma showed that the Hagedorn phenomenon indicates a phase transition. Dedicated lattice studies [41] have shown that the Hagedrorn temperature is above the critical temperatures, namely,

$$\frac{T_H}{T_c} \approx 1.11. \tag{11}$$

In the "Hagedorn regime" at T close to T_H both the energy and entropy $S = \ln N(L)$ are large, but in the free energy $F = E - TS$ the two terms cancel out, causing F to remain small. Since $F = -pV$, the string in the Hagedorn regime carries small pressure and does not explode. (Below we will further argue that near-critical strings should rather implode, due to their attractive self-interaction.)

The simplest derivation of T_H comes from "coarse lattice" estimate by Polyakov. Imagine a d-dimensional lattice with spacing $a \sim l_s$ and draw all possible strings of length L/a making all possible turns (except going backward) at each site, that is

$$N(E) \approx (2d-1)^{L/a} = e^{E(L)/T_H}, \tag{12}$$

where in the last term we changed length into energy using the string tension $E(L) = \sigma_T L$. This leads to

$$T_H = \frac{\sigma_T a}{\ln(2d-1)}, \tag{13}$$

but in practice this is used to estimate a rather than T_H.

Continuum strings lead to the expression

$$(T_H^{\text{QCD}})^2 = \frac{3}{D_\perp}\frac{\sigma_T}{2\pi} \approx (0.176\ \text{GeV})^2, \tag{14}$$

which is indeed close to the critical temperature of the QCD deconfinement-chiral restoration transition. In gluodynamics without quarks, there are no mesons and baryons containing fundamental strings. Glueballs are made of closed or double strings. The double string tension $2\sigma_T$ of such strings leads to a modified Hagedorn temperature,

$$T_H^{YM} = \sqrt{2} T_H^{QCD} \approx 0.237\ \text{GeV}, \tag{15}$$

which indeed approaches (but not matches) the lattice value mentioned above, namely $T_H^{YM} \approx 0.3$ GeV.

As the string density gets large enough, the Hagedorn regime ends at the point B of Fig. 6. This happens when the energy (entropy) densities become as large as

$$\frac{\epsilon}{T_H^4} \sim \frac{s}{T_H^3} \sim N_c^2. \tag{16}$$

In this regime, the number of stringy degrees of freedom become higher than in the gluon gas and the latter becomes the preferable phase. Thus, a second qualitative change happens: the supercritical state is the deconfined or QGP phase. It can, however, still be described in a stringy language, as we will discuss below.

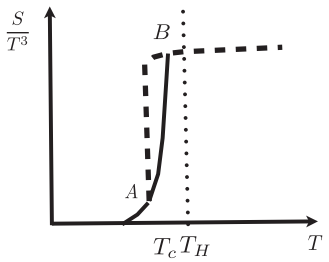

FIG. 6. Schematic temperature dependence of the entropy density. The dashed line represents equilibrium gluodynamics with a first order transition at $T = T_c$. The solid line between points A and B represents the expected behavior of a single string approaching its Hagedorn temperature T_H. The points A and B, separating the intermediate phase, are in correspondence with our notations in Fig. 1.

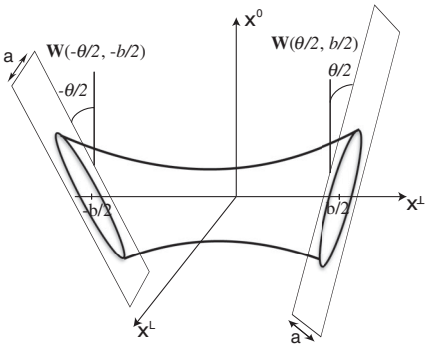

FIG. 7. Dipole-dipole scattering configuration in Euclidean space. The dipoles have size a and are b apart. The dipoles are tilted by $\pm\theta/2$ (Euclidean rapidity) in the longitudinal $x_0 x_L$ plane.

II. THE HOLOGRAPHIC POMERON

A. The SZ model

The holographic approach used in the SZ model is known as the "bottom-up" one. The holographic direction playing the role of the renormalization group scale, describing in particular the sizes of the through-going dipoles. There is a large N_c parameter used for book-keeping, a small string coupling g_s and a large 't Hooft coupling $\lambda = g_s N_c \sim 20$. (Subleading $1/\lambda$ effects of the curved geometry will be included only as a correction to the Pomeron intercept where small effects are important.) The setting includes AdS_5-like space with a confining wall where the important number of transverse directions is physically identified with

$$D_\perp = 3, \tag{17}$$

containing the transverse plane and the holographic direction. We refer to it as the SZ model. We note that its technical core—the calculation of the Euclidean amplitude of the twisted tube exchange shown in Fig. 7—was done in [5].

The main phenomenon to be studied is the string diffusion. At very high energies the standard large parameter,

$$\chi = \ln(s/s_0) \gg 1, \tag{18}$$

plays the role of an effective diffusion time.

We will now review the Pomeron results in this setting. The amplitude of the elastic dipole-dipole scattering reads [2,3,5]

$$\frac{1}{-2is}\mathcal{T}(s,t;k) \approx g_s^2 \int d^2\mathbf{b} e^{iq\cdot\mathbf{b}} \mathbf{K}_T(\beta,\mathbf{b};k), \tag{19}$$

where $\mathbf{K}_T$ is called the string (or Pomeron) propagator. One of its arguments, $\mathbf{b}$, is the impact parameter, which is the length of a "twisted tube," providing a semiclassical solution to the problem. The other argument β is the circumference of the tube. Its analogy with the Matsubara time leads to the introduction of an effective temperature T. Its value depends on the "diffusion time" χ and is also proportional to the impact parameter,

$$\beta = \frac{1}{T} = \frac{2\pi\mathbf{b}}{\chi}, \tag{20}$$

χ is our large parameter (18). The last integer argument k describes the color string flux, known also as N_c-ality and related to the Young tableaux of the color representations. In particular, for the antisymmetric ones k runs over all integers till $N_c/2$ for even N_c, and $N_c/2$–$1/2$ for odd ones. While we will show k in some formulas below, we will only use the usual string between fundamental charges (quarks) and $k = 1$, for the real world of SU(3) color. Only when we will need the large-N_c counting we will recall more general groups. Note that the first factor in the amplitude is the string coupling $g_s \sim 1/N_c$, small in the standard large-N_c counting.

The previous works such as [5] focused on what we would now call a "cold" regime of the string, namely a case

$$\mathbf{b} \gg \beta \gg \tilde{\beta}_H. \tag{21}$$

The former inequality follows from large collision energy (18) and the latter implies that the string is nearly straight, with small effective excitations (small effective T). The meaning of the tilde on the Hagedorn temperature (or the corresponding Matsubara time $\beta = 1/T$) will be explained below in (38). The explicit form of $\mathbf{K}_T$ was calculated in [5] using the Polyakov string action,

$$\mathbf{K}_T(\beta,\mathbf{b};1)=\left(\frac{\beta}{4\pi^2\mathbf{b}}\right)^{D_\perp/2} \times e^{-\sigma\beta\mathbf{b}(1-(\tilde{\beta}_H/\beta)^2/2)}\sum_{n=0}^{\infty}d(n)e^{2n\chi}. \quad (22)$$

The first combination of parameters in the exponents is the classical action. Here we emphasize the length $\beta/2$ or the semicircle, which first appeared in the semiclassical approach to pair production in an electric field process back in 1931 [42]. Note that we calculate the elastic amplitude in which a pair of virtually produced open strings makes a complete circle. This amplitude is the same as the cross section, or the modulus square of the inelastic amplitudes, with each corresponding to a tube cut in half, or two semicircles. Here $\sigma=\sigma_T/2$.

The first correction in the second line is due to the "thermal" excited states of the string: it corresponds to the so- called Luscher term in the string-induced potential. We wrote it using the (tilde) Hagedorn temperature of the double string (15). While physically in inelastic amplitude one produces an ordinary fundamental string, the conjugated amplitude has another antistring, making it into a double string. The last factor contains a summation over the integer n due to "tachyon string modes. In the Regge language those are called "Pomeron daughter trajectories. Some details of the weight $d(n)$ can be found in the Appendix A.

Inserting the leading $n=0$ contribution of (22) in (19) yields the Pomeron contribution to the elastic dipole-dipole scattering amplitude at large χ and fixed N-ality k,

$$\mathcal{T}(s,t;k)\approx ig_s^2\left(\frac{s}{s_0}\right)^{1+\frac{kD_\perp}{12}+\frac{\alpha' t}{2k}}. \quad (23)$$

Thus the resulting Pomeron has the intercept above 1 (and corresponds to a cross section growing with energy)

$$\alpha_{\mathbf{P},k}(0)=1+\frac{kD_\perp}{12} \to 1+\frac{kD_\perp}{12}\left(1-\frac{3(D_\perp-1)^2}{2kD_\perp\sqrt{\lambda}}\right), \quad (24)$$

where the second term is the Luscher contribution and the $1/\sqrt{\lambda}$ correction follows from the tachyonic correction (27) in curved AdS_5 [2].

While (22) has been derived in [5] from the semiclassical approach to a Polyakov string, but (to leading order in $1/\lambda$) it can be alternatively derived from a diffusion equation,

$$(\partial_\chi+\mathbf{D}_k(\mathbf{M}_0^2-\nabla_{\mathbf{b}}^2))\mathbf{K}_T=0, \quad (25)$$

where large χ interval is the time. The diffusion happens in the (curved) transverse space with the diffusion constant $\mathbf{D}_k=\alpha'/2k=l_s^2/k$. This diffusion (25) is nothing else but the Gribov diffusion of the Pomeron, leading on average to an impact parameter $\langle\mathbf{b}^2\rangle=\mathbf{D}_k\chi$ for close Pomeron strings. If the "mother dipoles:" are small in size, the diffusion is close to the UV end of the holographic coordinates and perturbative results are expected. For large times or dipole sizes, $\mathbf{b}$ is large and the string diffuses to the confining holographic region near the IR end of space, with a "confining wall." The "tachyon mass" is

$$\mathbf{M}_0^2=\frac{4D_\perp}{\alpha'}\left(\sum_{n=1}^{\infty}\frac{n}{e^{2\chi n/k}-1}-\frac{1}{24}\right). \quad (26)$$

The extra z coordinate is different from others. Note that the effects of the AdS_5 curvature is to make it difficult for the string to wander in the fifth dimension in the IR, effectively reducing the number of transverse dimensions and thus the Luscher contribution. To account for finite size dipoles, the string ends are placed at fixed heights z_1, z_2 a finite distance from the confining wall at z_0. As a result, the tachyon mass experiences corrections due to the curvature in z

$$\mathbf{M}_0^2\to\mathbf{M}_0^2+\frac{(D_\perp-1)^2}{4\alpha'\sqrt{\lambda}}. \quad (27)$$

Most of the arguments to follow will be carried out for large $\lambda\gg1$ unless indicated otherwise, so this effect is considered small.

The sub-critical string regime discussed so far is defined by the condition $\beta=2\pi\mathbf{b}/\chi>\beta_H$ in the diffusive limit $\langle\mathbf{b}^2\rangle=D_k\chi$. A more precise bound follows from the inclusion of the $1/\lambda$ corrections in the tachyon mass (27) or

$$\beta>\sqrt{2(\alpha_{\mathbf{P}}-1)}\beta_H \quad (28)$$

This leads to the bound $\chi<10$ for the corrected phenomenological value of the Pomeron intercept $\alpha_{\mathbf{P}}-1=0.08$ in (24), which roughly corresponds to energies below the LHC. This condition discriminates between a sub-critical and a critical string as we will detail below. We note that (28) implies a strong coupling renormalization of the Hagedorn temperature through the geometry of AdS_5.

B. Connecting to perturbative BFKL Pomeron

The Reggeon or Pomeron as an open or closed string exchange, can be viewed as a surface of multi-gluon exchanges. In weak coupling, the surface is dominated by rapidity ordered BFKL ladders [7].

The conformal nature of QCD perturbation theory as captured by the BFKL ladder re-summation can be recovered from the close string exchange since the AdS_5 geometry is conformal near the boundary. This point can be clearly seen in the holographic construction in curved AdS_5 by computing the density of wee partons $\mathbf{N}(\chi,z,c,r)$

(proportional to $\mathbf{K}_T$ in curved AdS [1]) of small size z sourced by a mother dipole of size r in the transverse radial coordinate space $r = \mathbf{b}$ for fixed rapidity χ. Specifically [1],

$$\mathbf{N}(\chi, z, c, r) \approx 2\frac{e^{(\alpha_{\mathbf{P}}-1)\chi}}{(4\pi\mathbf{D}\chi)^{3/2}}\frac{z}{cr^2}\ln\left(\frac{r^2}{zc}\right)e^{-\ln^2(\frac{r^2}{zc})/(4\mathbf{D}\chi)} \quad (29)$$

The diffusion is log-normal. The analogue of (29) in the context of onium-onium scattering was discussed in [43,44]. In particular, in the BFKL 1-Pomeron approximation it is given by [45]

$$\mathbf{N}^{\mathbf{BFKL}}(\chi, z, c, r) \approx 2\frac{e^{(\alpha^{\mathbf{BFKL}}-1)\chi}}{(4\pi\mathbf{D}^{\mathbf{BFKL}}\chi)^{3/2}} \times \frac{z}{cr^2}\ln\left(\frac{16r^2}{zc}\right)e^{-\ln^2(\frac{16r^2}{zc})/(4\mathbf{D}^{\mathbf{BFKL}}\chi)},$$

with the BFKL intercept $\alpha^{\mathbf{BFKL}}$ and diffusion constant $\mathbf{D}^{\mathbf{BFKL}}$

$$\alpha^{\mathbf{BFKL}} = 1 + \frac{\lambda}{\pi^2}\ln 2, \qquad \mathbf{D}^{\mathbf{BFKL}} = 7\lambda\zeta(3)/(8\pi^2) \quad (30)$$

Modulo the Pomeron intercept and the diffusion constant which are different (weak coupling or BFKL versus strong coupling or holography), the holographic result in the conformal limit is identical to the BFKL 1-Pomeron approximation.

The occurence of the $3/2$ exponent reflects on diffusion in $D_\perp = 3$. This point is rather important as it shows that the conformal nature of the QCD string is recovered if the QCD string evolves in curved AdS_5 instead of flat four-Minkowski dimensions. The curved and extra dimension captures the dipole scale evolution or equivalently the size of the closed string exchange during the collision.

C. Regge trajectories in SZ model

For completeness, we note that Reggeon exchange with open strings can be addressed similarly. For the Reggeon $\sigma = \sigma_T$ and the elastic scattering amplitude for dipoles of N-ality k is now

$$\mathcal{T}(s, t; k) \approx ig_s^2\left(\frac{s_0}{s}\right)\left(\frac{s}{s_0}\right)^{1+\frac{kD_\perp}{6}+\alpha' t} \quad (31)$$

with the extra s_0/s pre-factor accounting for the normalization of the spinors traveling on the exchanged world-sheet. This point was originally made in [9] but with different conclusions for the Reggeon intercept. At large s, the Pomeron exchange is dominant. The Pomeron as a closed string can be viewed as 2 glued open strings or a pair of Reggeons up to spin factors. As a result the Reggeon slope is twice the Pomeron slope while its intercept is also twice the Pomeron intercept.

A dual description of the scattering amplitude (19) is in terms of Pomerons and Reggeons in the holographic limit. Specifically,

$$\mathcal{T}(s, t) \approx ig_s^2(\pi a)^2\sum_{k=1}^{[N_c/2]}\sum_{n=0}^{\infty} \times \frac{(-1)^k}{k}\left(\frac{k\pi}{\ln s}\right)^{D_\perp/2-1} d(n)s^{1+\frac{D_\perp}{12k}-\frac{2n}{k}+\frac{\alpha' t}{2k}} \quad (32)$$

with all k N-alities included. The closed string or glueball trajectories following from (32) are

$$J \equiv 1 + \frac{D_\perp}{12k} - \frac{(D_\perp-1)^2}{8\sqrt{\lambda}} - \frac{2n}{k} + \frac{\alpha'}{2k}\mathbf{M}_{n,k}^2 \quad (33)$$

where the leading AdS_5 curvature correction is shown. We note that a proper P and C parity assignment for the glueball states follows from a Mellin transform of (32) and its parity conjugate. It will not be necessary for our discussion. For source dipoles in the fundamental representation or $k = 1$, the Pomeron trajectory corresponds to $\mathbf{M}_{0,1}^2$, while its daughters to $\mathbf{M}_{n>0,1}^2$. Their intercepts $\alpha_{P,D}(0)$ are tied by

$$\alpha_P(0) - \alpha_{Dn}(0) = 2n \quad (34)$$

while their common slopes are set by $\alpha'/2$. This is very consistent with lattice glueball Regge trajectories shown already in Fig. 5.

III. QUANTUM FLUCTUATIONS

A. The temperature and the entropy

Perhaps the use of the words "temperature", "entropy" etc should be in quotation marks, as the setting we discuss corresponds to the QCD vacuum at *zero* temperature. The reason is technical and originates from the fact that the exchanged strings have a world line—membrane of a shape of a tube shown in Fig. 3—quantized on a circle, with a periodic τ coordinate. This makes it formally identical to the thermal Matsubara formalism. Quantum string fluctuations take the form of thermal fluctuations. The temperature is the inverse of the tube circumference $T = 1/\beta$.

Furthermore, the tube circumference—and thus the effective string temperature—depends on the other world-sheet coordinate $0 \le \sigma_W \le 1$ [5]

$$T(\sigma_W) = \frac{\chi}{2\pi\mathbf{b}}\frac{1}{\cosh(\chi(\sigma_W - 1/2))} \quad (35)$$

with its highest value at the center or $T(1/2) \equiv T = \chi/2\pi\mathbf{b}$. It is instructive to focus on the actual effective temperature values, corresponding to LHC collisions. For

that we define a typical impact parameter $\mathbf{b}_{\rm eff}$ for pp collisions at energy s as

$$\mathbf{b}_{\rm eff}(s)=\sqrt{\frac{\sigma_P(s)}{\pi F_{\rm gray}}} \tag{36}$$

where $\sigma_P(s)$ is the Pomeron's part of the total pp and $\bar{p}p$ cross section [46], and $F_{\rm gray}<1$ is the factor which shows how "gray" is the nucleon. Inserting (36) into the effective temperature (20) yields Fig. 8. The effective temperature slowly rises with the collision energy. For gray or nonblack disc nucleons with $F_{\rm gray}<1$, the effective impact parameter is larger resulting into a downward shift in the effective temperature.

As we noted earlier in (24) the effects of the AdS_5 curvature causes effectively the string to move in effectively $\tilde{D}_\perp<D_\perp$ with

$$D_\perp\to\tilde{D}_\perp=D_\perp\left(1-\frac{3(D_\perp-1)^2}{2kD_\perp\sqrt{\lambda}}\right) \tag{37}$$

This translates to a higher effective Hagedorn temperature $\tilde{T}_H>T_H$ through (14) with

$$T_H^2\to\tilde{T}_H^2=\frac{3}{\tilde{D}_\perp}\frac{\sigma_T}{2\pi}\approx 1.8\ T_H^2 \tag{38}$$

where in the last equality we used a typical value $\lambda=20$, which gives $\tilde{T}_H\approx 0.224$ GeV.

The curvature-related corrections shift the effective Hagedorn temperature upward. The shift is close to the factor $\sqrt{2}$ one expects from the double-tension gluonic strings (as discussed in the thermodynamical introduction above). We may argue that the higher order curvature corrections perhaps shift it a bit more, to the critical temperature of the Yang-Mills theory $T_c\approx 0.27$ GeV or even beyond, it, to $T_H=1.11T_c$. Comparing those expectations with the effective temperature values calculated from the impact parameter in Fig. 8 we find that the exchanged string is expected to reach the near-critical regime only at collision energies well above the LHC domain. This justifies that so far most of the pp collisions are still described by a cold (far from critical) string. (However more central collisions lead to higher $T_{\rm eff}$ and the corresponding near and supercritical strings will be described in the next sections.) The thermal analogy allows us to define the free energy $\mathbf{F}=-\ln\mathbf{K}_T/\beta_U$ and the entropy corresponding to small string vibrations [2,3]

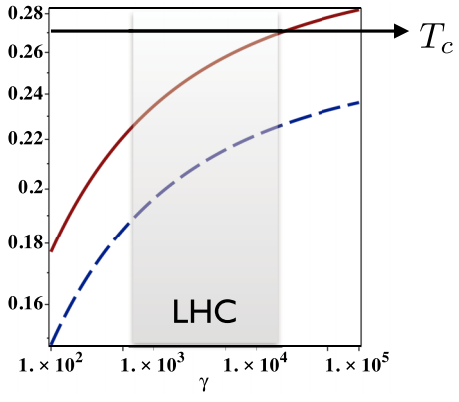

FIG. 8 (color online). The effective string temperature $T_{\rm eff}$ (GeV) versus the c.m. beam gamma factor γ. The curve for the black disc estimate $F_{\rm gray}=1$ is shown by the solid line, and for $F_{\rm gray}=0.7$ by the dashed line. The effective temperature is compared to the critical temperature T_c of *gluodynamics*, shown by a horizontal line with an arrow, which is related with the Hagedorn temperature by relation (11).

$$\mathbf{S}=-D_\perp\sum_{n=1}^{\infty}\left(\ln(1-e^{-\beta_k n})+\frac{\beta_k n}{e^{\beta_k n}-1}\right)+D_\perp\left(\frac{\beta_k}{12}-\frac{1}{2}\left(1+\ln\left(\frac{\beta_k}{2\pi}\right)\right)\right) \tag{39}$$

At large collision energy $\chi\gg 1$ the entropy is dominated by the last term due to the tachyon, so

$$\mathbf{S}\approx\frac{D_\perp\beta_k}{12} \tag{40}$$

Since $\beta_k=2\chi/k$ the entropy scales with the rapidity interval χ. In contrast, the energy $\mathbf{E}\approx\sigma\mathbf{b}$ with on average $\langle\mathbf{b}^2\rangle\approx\mathbf{D}_k\chi$, scales with the root of χ, and therefore is subleading for asymptotically large χ. This is a major difference between the "cold" regime and the others that we will discuss below.

For clarity, let us emphasize that this entropy characterizes the number of states of the "tube", or strings produced at the initial virtual stage of the collision. It is obviously *not* the number or states or entropy physically produced in the collision and observed in the detector, although we will argue below that there is a positive correlation between the two, at least in some regimes.

IV. NEAR-CRITICAL STRINGS

So far we have discussed the so-called "minimally biased" collisions. Their typical impact parameter was extracted from the total cross section. Now we switch to discussing certain fluctuations in a system, corresponding to more "central" collisions, with the impact parameter smaller than the typical one. (At this point the reader may ask how experimentally one can find such an event. We postpone its discussion to Sec. VI below.)

A. The Hagedorn phenomenon leads to string balls

As it is clear from the formulas given above, the smaller impact parameters correspond to thinner tubes and thus higher effective temperatures. The central idea of this paper

is that some radical change is expected when the effective string temperature approaches the Hagedorn temperature $T \to \tilde{T}_H$ (the tilde is a reminder of the curvature corrections). The string fluctuations change from small as shown in Fig. 9a, to large as shown in Fig. 9b. The reduction of the effective string tension leads to a proliferation of string fluctuations. The energy of the string and its entropy grows, as the effective temperature T approaches $\tilde{T}_H$. We will argue that in this case a string generates a massive cluster, to be called a "string ball" below. The physical analogy to what happens in the thermal (heat bath) setting is at the origin of this idea.

Now, is there any connection between the effective thermodynamics of the virtual exchanged string we discussed above, and the multiplicity of the produced hadrons? The initial string configuration we discuss in connection with the elastic amplitude does not of course directly correspond to the physical final states. Two open strings make a virtual (under the barrier) semi-circle and are then born into the physical Minkowski world as a pair of real strings thanks to the Schwinger pair production mechanism. Their virtual Euclidean evolution ends there. The subsequent evolution in Minkowski signature happens with probability one and thus is irrelevant for the scattering amplitude. It is not described by the formalism we use.

Yet, at least in the near-critical regime, one may argue that the large energy and entropy of the string-ball cluster is simply proportional to the physical length of the string. These strings are to be stretched longitudinally, and then broken into pieces, corresponding to physical mesons whose multiplicity we trigger. While those phenomena are complicated (and described by phenomenological models, e.g. those originating from the Lund model), we may still argue that the final multiplicity should grow with the length of the initial but virtual string. Furthermore, we think that the final multiplicity should simply be proportional to the initial length of the string, to its energy or entropy.

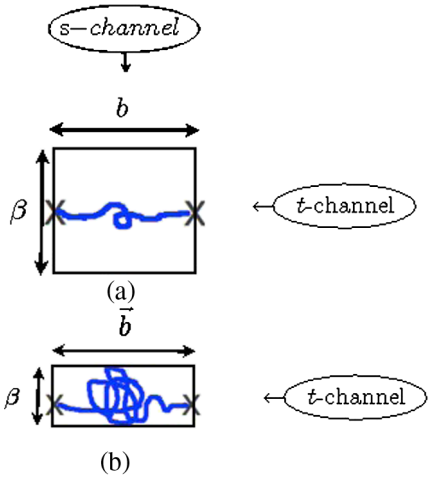

FIG. 9 (color online). String exchange between two sources (crosses) separated by the impact parameter **b**: the cold string case $\beta < \beta_H$ (a); the near-critical string ball $\beta \to \beta_H$ (b).

The theoretical description of the near-critical strings can be made in the so-called "thermal scalar" formalism, suggested in [47] (and used e.g. in [48] to be discussed in the next section). The meaning of this complex scalar field φ is a coefficient of certain string wrapping modes with a mass

$$m_\varphi^2 = \frac{\beta^2 - \beta_H^2}{4\pi^2(\alpha')^2} \tag{41}$$

vanishing at the Hagedorn point. A free field with such a mass corresponds to a free (random walk) string with a Gaussian diffusive distribution. The description of the free string ball in the near-critical random walk (r.w.) regime is covered in detail in [48]. Let us just mention that its radius depends on the number of "turns" N and thus the mass as

$$\frac{R_{r.w.}}{l_s} \sim \sqrt{\frac{L}{a}} \sim \sqrt{M} \tag{42}$$

for any dimension d.

B. Self-interacting string balls and black holes

When any object gets very massive, it is amenable to a classical description. Sufficiently massive string balls should become black holes. String theorists have studied exactly how the interpolation between the states of massive string balls and those of black holes happen.

Let us start with naive estimates, which will elucidate the problem. The string ball can be seen as a random walk made of M/M_s steps, with $M_s \sim 1/\sqrt{\alpha'}$ the typical mass of a segment. The string entropy is the number of segments

$$S_{\text{ball}} \sim \frac{M}{M_s}. \tag{43}$$

The Schwarzschild radius of a black hole in d spatial dimensions is

$$R_{\text{BH}} \sim (G_N M)^{\frac{1}{(d-2)}}, \tag{44}$$

and the Bekenstein entropy

$$S_{\text{BH}} \sim \frac{\text{Area}}{G_N} \sim \left(\frac{M}{M_s}\right)^{\frac{d-1}{d-2}} \tag{45}$$

grows with the mass as a power less than 1. Thus their equality $S_{\text{ball}} = S_{\text{BH}}$ can only be reached at some special mass. This happens when the Hawking temperature of the black hole is exactly the string Hagedorn value T_H and the radius is at the string scale. So, at such mass a near-critical

string ball can be identified—at least thermodynamically—with a black hole.

However, in order to understand how exactly it happens one should first address the following puzzle. The random walk radius (42) does not agree with the Schwarzschild radius $R_{\rm BH}$ given the above (44); e.g., the former does not depend on space dimension d and the latter does. So, something important has been missing, since a smooth interpolation to the black hole properties has not yet been achieved.

This goal has been reached in two steps. We believe Susskind first pointed out the importance of string self-gravity, and the consequent contraction of the ball size. Horowitz and Polchinski [48] used mean field analysis, and Damour and Veneziano [49] (whom we follow below) completed the argument by using the correction to the ball's mass due to self-interaction. Their reasoning is as follows: self-interaction causes a shift in the string mass

$$\frac{\delta M}{M} \sim -\frac{g^2 M}{R^{d-2}} \tag{46}$$

where g is the string self-coupling constant. We changed self-gravity to self-interaction because in the AdS/QCD setting the attraction due to the scalar dilaton field is as important as gravity. (In the quoted expression above, this amounts to a coefficient change, which is suppressed anyway.)

Omitting some technical points we proceed to the expression for the entropy of a self-interacting string ball of radius R and mass M,

$$S(M,R) \sim M\left(1-\frac{1}{R^2}\right)\left(1-\frac{R^2}{M^2}\right)\times\left(1+\frac{g^2 M}{R^{d-2}}\right), \tag{47}$$

where all numerical constants are suppressed for brevity. For very weak coupling the last term in the last bracket can be ignored and the entropy maximum is given by the first two terms. This brings us back to a random walk string ball. However, even for very small g, the importance of the last term depends not on g but on gM. So, a very massive balls can be influenced by a very weak self interaction (as indeed are planets and stars). If the last term is large compared to 1, the self-interacting string balls are much smaller in size than the naive random walk estimates suggest.

What exactly happens depends somewhat on space dimension d. Plots for $d=3$ (four-dimensional space-time) and varying coupling are shown, as examples, in Fig. 10. As one can see, a free (random-walk) string at zero coupling has a maximum in the middle of the plot. As self-coupling grows, the string ball basically implodes, reducing its most likely radius. One can also see that it smoothly interpolates eventually to the Schwarzschild radius of a black hole. Numerical studies of self-interacting string balls will be reported elsewhere [50].

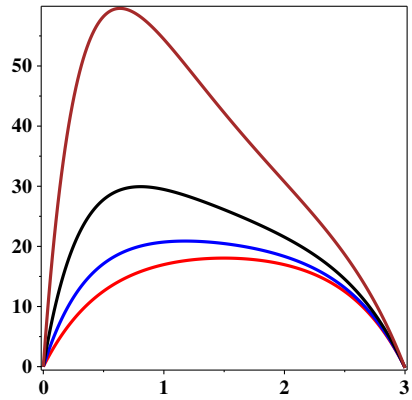

FIG. 10 (color online). The entropy $S(M,R)$ as a function of $\log R$ for $M=20$, $d=3$. Four (red,blue,black and brown) curves, bottom-to-top, are for the string self coupling $g=0$, 0.03, 0.1, 0.3. The corresponding shift of the maximum is from a free string ball to a black hole.

To summarize: in the near-critical regime one finds self-interacting string balls, or string holes, which combine a growing energy and entropy of a cluster with the implosion of its size due to self-interaction. It is such objects which dominates the near-critical "mixed phase" of QCD and scattering at intermediate impact parameters.

The detailed consequences of this scenario for AdS/QCD models or QCD strings remain to be worked out. In the latter case an important ingredient of the problem is the finiteness of the scalar and tensor glueball masses. A Yukawa-like potential would substitute to the Coulombic corrections stemming from a massless dilaton and graviton of the string theory. This clearly would somewhat reduce the collectivity of the phenomenon. We plan to report studies of such string balls elsewhere.

C. The scattering amplitude in the near-critical regime

Let us now see how the scattering amplitude and other properties of the string change as one enters this new "near-critical" regime. Recall first the expressions discussed above, such as (22), which were derived using the Polyakov action in the regime $\tilde{\beta}_H < \beta < \mathbf{b}$. They were dominated by the ground state mode $n=0$, so

$$\mathbf{K}_T(\beta,\mathbf{b};1) \approx \left(\frac{\beta}{4\pi^2\mathbf{b}}\right)^{D_\perp/2} e^{-\sigma\beta\mathbf{b}(1-\tilde{\beta}_H^2/2\beta^2)}. \tag{48}$$

However, as the effective temperature becomes closer to the Hagedorn temperature $\beta\to\tilde{\beta}_H$, the string excitations are no longer small and the $(\tilde{\beta}_H/\beta)^n$ corrections with all n need to be resummed.

The resummed result follows in the spirit of Arvis [40] already mentioned and takes also a square root form (we start with the $n=0$ case, returning to other terms later),

$$\mathbf{K}_T(\beta,\mathbf{b};1)\approx\left(\frac{\beta}{4\pi^2\mathbf{b}}\right)^{D_\perp/2}e^{-\sigma\beta\mathbf{b}(1-\tilde{\beta}_H^2/\beta^2)^{1/2}}. \quad (49)$$

Clearly (49) reduces to (48) for $\tilde{\beta}_H/\beta\ll 1$. The first correction is the analogue of the "Luscher" term. This and all other corrections have sign plus, so that each of them increase the amplitude, as we indicated in our sketch Fig. 1 near the point A.

Another way to say it is that the resummed expression (49) corresponds to the effective string tension to vanish at the Hagedorn point,

$$\sigma(1-\tilde{\beta}_H^2/\beta^2)^{1/2}\to 0, \quad (50)$$

in agreement with the universal behavior observed for strings in a heat bath. As we noted above, this occurs when the impact parameter $\mathbf{b}\approx\chi l_s$.

Now we generalize it to any n,

$$\sum_{n=0}d(n)\exp\left(-\sigma\beta b\sqrt{1-\frac{\beta_H^2}{\beta^2}+\frac{4n\chi}{\sigma\beta b}}\right), \quad (51)$$

again using the idea that the term under the root is uniquely defined via its first correction known before.

Changing e^{-n} to $e^{-\sqrt{n}}$ changes the convergence of the sum. Furthermore, since at high n the density of states behaves as $e^{\sqrt{n}}$ (A2), one finds another instance of the Hagedorn phenomenon, in which suppression of the Pomerons' daughters will be lifted by the growing density of states $d(n)$. As one can see in Fig. 11, for smaller $\mathbf{b}$ the sum over n diverges. However, we should disregard this second Hagedorn point because it lies in the region of $\mathbf{b}$ to the left of the vanishing string tension for $n=0$. Indeed in this case we are in a different supercritical phase, to be discussed below, and the expression used is not valid.

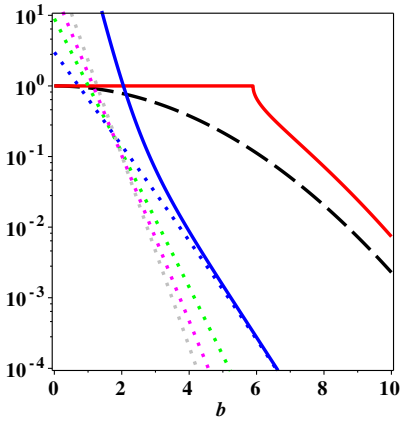

FIG. 11 (color online). Example of b dependence of scattering amplitude. The (black) dashed line is the original Gaussian, the (red) solid line with a kink is the resummed version (51), four dotted curves are terms in the sum for $n=1$, 2, 3, 4, and (blue) solid line rising to the left is the sum with exact $d(n)$.

The scattering amplitude associated to such regime can be obtained by inserting (49) in (19). The result in the saddle point approximation reads

$$\mathcal{T}(s,t;1)\approx ig_s^2\left(\frac{s}{s_0}\right)^{(t/\sqrt{2})(1-\frac{1}{4}(1+\sqrt{1-2/t}))(1+\sqrt{1-2/t}+1/t)^{1/2}}. \quad (52)$$

In this expression t is in string units, so actually it is $\alpha' t$, and $k=1$. This expression (53) reduces to the Pomeron amplitude (23) for $s\gg -t>1/\alpha'$. One may in principle observe the corresponding modifications in the elastic scattering. However, we think this to be only possible at energies well above the LHC, so we will not elaborate further on this point.

V. THE SUPERCRITICAL REGIME

A. Strings with condensed "thermal scalar"

As we emphasized above, at $T>T_c$ the string ball simply turns into a ball of plasma, which can be described in terms of deconfined colored quasiparticles, gluons and quarks. Even as we know the interaction in this matter, known as sQGP, remains strong, its approximate conformal symmetry requires the pressure to be no longer subleasing, but instead jump to the conformal value $p=\epsilon/3$. The consequences of this fact is the "explosive" behavior to be discussed later. From a theoretical perspective, the simplest option is that the "most central" supercritical collisions should be described via perturbative QCD, e.g., by the BFKL Pomeron scattering amplitude, and thus forget about confinement and strings in this regime.

However, one can proceed into the deconfined phase with a string-based description as well. An important notion, well known to string theorists, is that a string can be viewed as infinitely many fields that are technically the coefficients of the vibrational modes.

One approach to the supercritical region is to follow the "thermal scalar" formalism [47] already discussed. Naively, the mass square of the field φ (41) gets negative. As usual, it means that zero mean of that field is unstable and that it develops a nonzero condensate $\langle\varphi\rangle\neq 0$. Its magnitude is determined by higher order terms, usually by the positive quartic term $|\varphi|^4$ in the effective Landau-Ginzburg action. As a result, a shifted field $\varphi-<\varphi>$ has positive mass. The correlator of two masses becomes of the type

$$\langle|\varphi(0)|^2|\varphi(x)|^2\rangle=|\langle\varphi\rangle|^4+\mathcal{O}(e^{-|x||M_\varphi|}). \quad (53)$$

This phenomenon is also known as the formation of a nonzero Polyakov's "disorder parameter" at $T>T_c$ in finite temperature QCD.

But a more direct and more physically appealing description is the holographic one. Since the supercritical regime corresponds to a trapped surface (black hole) formation, one should rethink any string-induced amplitudes: parts of the strings inside the horizon should not be counted. (See Fig. 2 for a picture.) This explains why charges are no longer connected to each other but "liberated." The part inside the BH cannot transmit any information outside, thus strings effectively end on the horizon: so (in the leading order) there is no potential between the charges, as the factorized result (53) tells us.

The lesson of this section, once again, is that there is a fundamental asymmetry between the perturbative and the stringy points of view. Why we don't know how to derive strings and thus the confining phase from a perturbative viewpoint, one can provide a relatively simple and logical description of the perturbative domain starting from strings, even through the deconfinement phase transitions.

VI. THE OBSERVABLES

A. Elastic scattering

Earlier in our discussion in the Introduction we have defined a "profile function" $F(s,\mathbf{b})$ in (2) related to the scattering amplitude as its Bessel transform. Now we tie this to the proton wave functions. In so far as we have considered fixed-size dipoles, the proton as a quark-diquark can be viewed as a dipole. However, the dipole size fluctuates inside the proton wave function. With this in mind, we now identify the curved fifth coordinate z with the dipole size. Using the scale-free coordinate $u=-\ln(z/z_0)$ with $z_0>z$ or $u>0$, the coordinate of the confining wall, we define

$$F(s,\mathbf{b})=\int du_1 du_2 \times |\Psi(u_1)|^2|\Psi(u_2)|^2 K(u_1,u_2,\mathbf{b},s). \quad (54)$$

Because of the fluctuations, the two dipole sizes are different in general. The ensuing formulas are therefore a bit more involved. The string propagator K connects two points in the curved three-dimensional transverse space, say $(-\mathbf{b}/2,u_1)$, $(+\mathbf{b}/2,u_2)$. Much like bulk propagators, K can be simply expressed in terms of a combination of arguments involving the "chordal distance" ξ in curved AdS between these two points. Specifically,

$$\cosh(\xi)=\cosh(u_2-u_1)+\frac{1}{2}\frac{\mathbf{b}^2}{R^2_{\rm ADS}}e^{u_1+u_2}, \quad (55)$$

where $R_{\rm ADS}$ is the radius of the effective space (in GeV^{-1} and similarly for $\mathbf{b}$). Since the AdS space is walled at z_0, there is a reflected propagator. The invariant "chordal distance" ξ_* is set by the image and reads

$$\cosh(\xi_*)=\cosh(u_2+u_1)+\frac{1}{2}\frac{\mathbf{b}^2}{R^2_{\rm ADS}}e^{u_2-u_1}. \quad (56)$$

The string amplitude derived in [4] indeed takes a more intuitive diffusive form in such variables,

$$K(u_1,u_2,\mathbf{b},s)=\frac{g_s^2}{4}(2\pi\alpha)^{3/2} \times(\Delta(\chi,\xi)+e^{2u_1}\Delta(\chi,\xi_*)), \quad (57)$$

$$\Delta(\chi,\xi)=\frac{\exp[-\frac{\xi^2}{4D\chi}+\chi(\alpha_P-1)]}{4\pi D\chi}\frac{\xi}{\sinh(\xi)}, \quad (58)$$

with $D=1/2\sqrt{\lambda}$ and $\alpha_P-1=1/4$. This corresponds to a "tube amplitude" with small excitations, which is to be applicable at very large $\mathbf{b}$.

For intermediate $\mathbf{b}$, we follow the arguments in Sec. IV C and generalize (57) to the near-critical regime by the Arvis-style substitution of the first two terms to full square root containing all higher-order Nambu string corrections,

$$-\frac{\xi^2}{4D\chi}+\chi(\alpha_P-1)\to-\frac{\xi^2}{4D\chi}\left[1-\frac{\tilde{\xi}^2}{\xi^2}\right]^{1/2}, \quad (59)$$

where $\tilde{\xi}=\chi\sqrt{8D(\alpha_P-1)}$.

To streamline the numerical analysis of the profile function in the near-critical regime, we now make some bold simplifications: (i) ignore the reflection term, (ii) include the distance-independent amplitude at small ξ in the supercritical regime, and (iii) fix the overall normalization constant in such a way that at the point of the vanishing square root $K=1$. This results in a relatively simple expression,

$$K(u_1,u_2,\mathbf{b},s)\approx e^{-\frac{\xi^2}{4D\chi}\mathrm{Re}\sqrt{1-\frac{\tilde{\xi}^2}{\xi^2}}}. \quad (60)$$

If the dipole sizes u_1, u_2 are fixed and equal, the profile has the shape shown in Fig. 12 by the dashed line. Note the singularity corresponding to the end of the intermediate regime and the beginning of the black hole formation (called in some previous plots point B). Such a singularity —or a jump in the function following the first-order transition in string thermodynamics—in the scattering profile would not be phenomenologically acceptable. Its Bessel transform would generate a too small power of t in the differential cross section $d\sigma/dt$ at large t.

However, it is expected on general grounds (and also known experimentally from diffraction) that nucleons are strongly fluctuating, from one event to the other. In our approach the nucleon is simplified to a color dipole (between a valence quark and a diquark). Its fluctuations are described by the wave function in the fifth dimension $\Psi(u)$. Making various shapes and widths of this function

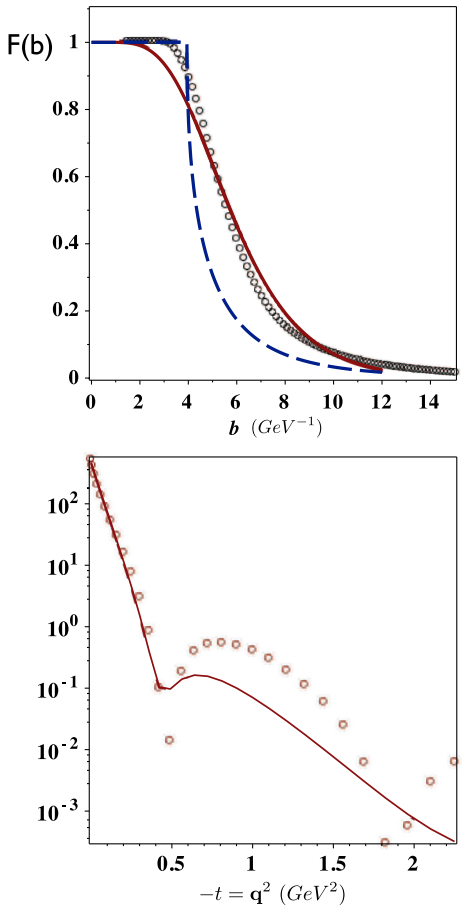

FIG. 12 (color online). The profile function $F(\mathbf{b})$ versus the impact parameter $\mathbf{b}$ is shown in the upper plot for LHC $\sqrt{s} =$ 7 TeV energy. The solid line is the same curve as in Fig. 4 corresponding to the BSW data parametrization. The dashed line is the shape corresponding to the approximation (59) for fixed sizes of the dipoles $u_1 = u_2$, while the circles correspond to the profile with the fluctuating dipoles. The lower plot shows the corresponding absolute value squared of its Bessel transform as a function of momentum transfer.

and performing the averaging over the string endpoints u_1, u_2, we got profiles in between the dashed line (at small fluctuations) to the shape shown by circles in Fig. 12, for large $\mathcal{O}(1)$ fluctuations of the dipole sizes. While the resulting profile is rather close to the BSW parametrization of the data, the modulus squared of its Bessel transform (shown in the lower part of Fig. 12) shows more visible differences. The dips, in particular, are much more pronounced. The reason is that our model contains only the imaginary amplitude, while the BSW data parametrization has the real part as well. Since this paper is about qualitative effects, we have not tried to make more sophisticated shapes of the string propagator which would fit the $d\sigma/dt$ TOTEM data better. See also [4] for a similar fit using fixed dipole wave functions. The shape (60) is of course a caricature, with a square root singularity. All we want to emphasize is that it corresponds to the end of the Hagedorn transition and approximately describes the structure seen in the elastic amplitude profile.

B. The final state of inelastic collisions

Stricktly speaking, this subject goes beyond the content of the present paper, as we have only analyzed the Euclidean part of the system path. Still we would like to make some general comments.

The perturbative approach to the Pomeron, based on resumming gluon ladders, was studied both at the level of the elastic and inelastic amplitudes. Feynman diagrams can be "cut" by the well-known unitarity rules, predicting single-gluon and two-gluon distributions in the inelastic collisions. However, at small $|t|$ we cannot justify perturbative methods. While the use of strong coupling λ and large N_c yield "fishnet diagrams" resembling a string world sheet, the correspondence was never made sufficiently precise.

Our approach uses from the start a string description (strong-coupling). The elastic amplitude, in particular, was calculated using an under-the-barrier "tube," virtual string exchange, resulting in the "holographic Pomeron" described above. In principle, we could have followed the system, from its Euclidean birth to its Minkowski evolution, and calculated the string configurations, all the way to their final breaking and hadronization. We plan do to so elsewhere.

Nevertheless, we would like to speculate on this issue, arguing that some properties of the virtual string should find their way to observable final states. As is well known from experiment, final hadrons—mostly pions—come from certain clusters, hadronic resonances. Those are well described by the Lund-type model, including string breaking into certain segments, before final decays into pions. Our conjecture is that in the high-multiplicity events associated with string balls as we detailed above, these clusters are perhaps larger.

In standard Regge phenomenology, one uses the so-called Kancheli-Muller diagrams [51] (see Fig. 13) to calculate the single and many-hadron spectra. We focus now on the two-particle correlations. From the t-channel point of view, (nearly) unclustered two-particle spectrum corresponds to the Pomeron exchange, and further clustering corresponds to "daughters" of the Pomeron with $n > 0$

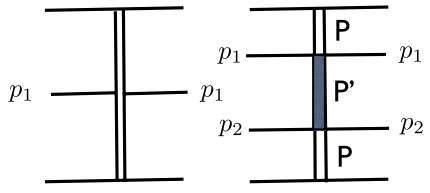

FIG. 13 (color online). Mueller-Kancheli diagrams for single and double particle production from Pomeron exchange. In Fig. 2 the shaded region indicates the excited Pomeron P'.

excitations. The lines in Fig. 13 are the corresponding propagators, which we do know. They naturally satisfy the usual relations, in which a propagator can be written as a convolution of two propagators, integrated over the intermediate points. So we attempt now to use those, in the spirit of Kancheli-Mueller rules, in an attempt to describe clustering. Including the leading Pomeron and its first daughters to the two-particle correlations, one expects the following rapidity dependence:

$$\frac{dN}{d\Delta y} = C_P e^{\Delta y(1-\alpha_P(0))} + C_{P'} e^{\Delta y(-\Delta\alpha_1)} + \ldots. \quad (61)$$

The second contribution stands for the first daughter, while the dots for the higher daughters. Note that the Pomeron has an empirical intercept of 1.08–1.20, making the first contribution slightly rising with the rapidity interval, as is indeed observed. The "Pomeron daughter" contribution rapidly decreases with the rapidity interval since the difference of intercepts is large (4).

The two particle correlation functions in the high multiplicity events are measured by the CMS Collaboration, although publicly available data are quite limited. The peak at small $\Delta\eta$ is usually interpreted as "jet-generated." We doubt this to be the case since it is well seen at small $p_t \sim 1-3$ GeV where jet contribution is small.

Somewhat surprisingly, the approach based on t-channel exchanges works well, even for high multiplicity events. In Fig. 14 we show the experimental data on the two-particle rapidity distribution from CMS which we fitted as a function of Δy. The fit suggests $\Delta\alpha_1 = 2.2 \pm 0.2$, which is in the vicinity of the value (4) obtained by the Regge extrapolation of the lattice glueball data. The most notable feature of this fit is the fact that the coefficient of the "Pomeron daughter" is larger by a factor ~30 than that of the leading Pomeron. We take it as the first direct confirmation of a large cluster production in high multiplicity events. Such a strong

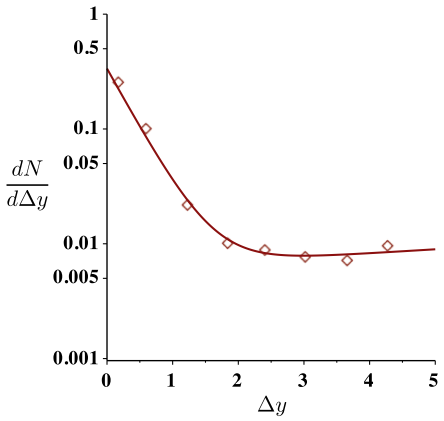

FIG. 14 (color online). Two particle correlation function fitted to P and P' exchanges (61). The points are from the CMS data, Fig 2 of [52], for the high multiplicity bin $N > 110$ and $2 < p_\perp^{\rm trig} < 3$ GeV, $1 < p_\perp^{\rm assos} < 2$ GeV.

enhancement of the subleading Pomeron is also supported by our holographic estimate (34). To summarize this point, we suggest that the so-called "jet-peak" structure seen in two-particle correlators is actually a hadronic cluster originating from a string ball. Its dependence on multiplicity should be studied systematically.

This suggestion should of course be tested further. The peak is not only in the rapidity Δy variable, but it also has a certain shape in azimuthal angle $\Delta\phi$. At this time, we have not analyzed whether this shape can or cannot be described by the exchanged Pomeron and its daughters.

Another prominent observed structure is the so-called away-side peak at $\Delta\phi \approx \pi$. At large $p_\perp$ this is ascribed to di-jet events. At smaller $p_\perp$ the away-side balances kinematically the trigger particle. If the Pomeron is described perturbatively, via gluon ladders in weak coupling, then the back-to-back correlations are natural. In central pA collisions those are enhanced, and a quantitative discussion of this effect is available due to Dusling and Venugopalan [53]. As shown by those and other authors, gluon diagrams also generate certain elliptic asymmetry v_2, as the impact parameter direction is dynamically different from the other transverse direction.

Let us at the end of this section suggest another interpretation, based on our view of a cluster remnant of the string ball produced at the initial time. As is clear from Fig. 2, the tension of the string ends pulled along both beam directions should supply the ball with angular momentum J normal to the beam and the impact parameter. Since J is conserved in the cluster decays, the products would carry it away, making the distribution anisotropic in azimuth (enriched in the impact parameter direction).

C. Explosions of the supercritical fireball

We already mentioned the pressure of the QGP $p \approx (1/3)\epsilon$. A very important consequence of this pressure is that the fireball explodes. While the details of such phenomenon are already well studied via heavy ion (AA) collisions, it still came as a surprise to many that in pp and pA collisions very high multiplicity events can indeed display collective explosion. The now famous "ridge" is now interpreted as a hydrodynamical elliptic flow. Higher azimuthal harmonics of the flow also have been studied, and they are also surprisingly well described by hydrodynamics.

However, azimuthal harmonics are just relatively small deformations of the hydro flow: the main effect is the so-called radial flow (in the transverse plane). It has been predicted in version 1 of our paper [6] that the radial flow in pp and pA should exceed in magnitude that previously observed in AA collisions. Very recently this prediction has been confirmed by CMS and ALICE Collaborations, as they have measured the spectra of identified secondaries (π, K, p, Λ etc) (see version 2 of that paper as published [6]).

A relatively small size of the fireball produced at freeze-out, together with a strong radial flow, leads to a conclusion

that it must start with an extremely small and dense initial state. This correlates well with the attractive string self interaction and its tendency to implode (dual to gravitational collapse). Thus the explosion that follows may look puzzling. The answer is that it is not the string ball which explodes, but the Hawking radiation created by its horizon. Naturally it only happens if it is massive enough. So one expects to find a certain threshold in multiplicity.

Unfortunately an estimate of the corresponding critical multiplicity (above which an explosion should happen) is not so straightforward. We can calculate the entropy of the string, as it leaves the Euclidean (under-the-barrier) part of its path, but we do not describe its further evolution in the Minkowski world, including its fragmentation into the observed hadrons. While this evolution does not change the probability of the process, it generates new entropy.

Let us suggest two arguments to this point. The first argument is a lower bound. Since the entropy never decreases, the string-ball entropy should provide a lower bound on the final entropy and thus the multiplicity. The critical multiplicity $\mathbf{N_c}$ associated with the explosion of the black-hole is limited by entropy near the Hagedorn temperature,

$$\mathbf{N_c} > 7.5\mathbf{S} \approx \sigma\beta_H \mathbf{b}(1-\tilde{\beta}_H^2/\beta^2)^{-1/2}, \tag{62}$$

where the conversion factor of 7.5 is borrowed from the entropy-to-hadron density relation at freeze-out. Substituting $\tilde{\beta}_H/\beta - 1 \approx 1/N_c$ in (62), we find the critical charge particle multiplicity to be

$$\mathbf{N_C} > 7.5\chi/2 \approx 50. \tag{63}$$

This bound (63) surprisingly agrees with the measured threshold charge tracks multiplicity of $N > 50$ for events with the ridge, according to the CMS Collaboration [17]. The agreement is however purely accidental. If one includes the actual acceptance of the CMS detector in $p_\perp$, as well as include a factor 1.5 for neutral secondaries, the actual multiplicity is larger than the CMS track count by about a factor of 3.

The second argument is that since string fragmentation is essentially a local process, the resulting multiplicity is proportional to the string length. Since in the near-critical regime the string entropy is proportional to its length as well, we suggest that the string entropy we calculate and the final multiplicity should be, in this regime, proportional to each other.

VII. THE STRING BALL AS AN EFFECTIVE BLACK HOLE

This section contains some additional theoretical material, which is not necessary for the overall understanding of the rest of the paper. However, it provides interesting alternative physical analogies and results. In it we will show that the string-ball state is thermodynamically (and perhaps in other respects) dual to a BH.

The colliding protons viewed as dipoles are depicted in the cartoon of Fig. 2 as beam 1,2. They fly along the longitudinal direction x^1 which is Lorentz contracted. The exchanged closed string as a diffusive ball is shown also in Fig. 2. The string ball forms in the transverse volume span by $x^{2,3}$ and z with a wall at z_0. This string ball is the precursor of the string black hole. Its volume is set by the string diffusion scale $\sqrt{\chi/k}l_s$ along $x^{2,3}$ and $\min(\sqrt{\chi/k}l_s, z_0)$ along the holographic z direction. We now make some of these statements more quantitative.

The near-critical string has a propagator (49) that behaves like a thermal ensemble with Unruh temperature $1/\beta_U$. Its free energy or pressure $\mathbf{F} = -\ln\mathbf{K}_T/\beta_U$ [2] is small,

$$\mathbf{F}(\beta, \mathbf{b}) \approx k\sigma\mathbf{b}\left(1-\frac{\tilde{\beta}_H^2}{\beta^2}\right)^{1/2}, \tag{64}$$

but its energy and entropy are large,

$$\mathbf{E} = \partial_{\beta_U}(\beta_U k\mathbf{F}) \approx k\sigma\mathbf{b}\left(1-\frac{\tilde{\beta}_H^2}{\beta^2}\right)^{-1/2}$$
$$\mathbf{S} = \beta_U^2\partial_{\beta_U}\mathbf{F} \approx (\tilde{\beta}_H^2/\beta)k\sigma\mathbf{b}\left(1-\frac{\tilde{\beta}_H^2}{\beta^2}\right)^{-1/2}. \tag{65}$$

For $\beta \approx \tilde{\beta}_H$ this coincides with the first law of thermodynamics for black holes in Rindler coordinates as noted by Susskind [54],

$$\mathbf{S} \approx \beta_H \mathbf{E} = 2\pi(\mathbf{E}l_s), \tag{66}$$

and vanishingly small pressure (64). We note the Rindler temperature $T_R = 1/2\pi$ and therefore the Rindler energy $\mathbf{E}_R = \mathbf{E}l_s$. The emergence of a Rindler temperature is expected since the stringy Pomeron exchange is characterized by a line element [2]

$$ds^2 \approx -a^2\rho^2 dt^2 + d\rho^2 + ds_\perp^2, \tag{67}$$

with a Rindler acceleration $a = \chi/\mathbf{b}$. At this regime the acceleration is $a = k/l_s$. On the stretched horizon at $\rho = l_s/k$ in (67), the warping of time is 1 since $t/t_\rho = (b/\chi)/\rho \to l_s/k\rho$. A cartoon of the string ball as a black hole is shown in Fig. 2.

The transverse area of the black hole is the area of the diffusing string in rapidity,

$$A_{\mathrm{BH}} = 2\pi^2(\sqrt{\chi/k}l_s)^3, \tag{68}$$

in transverse $D_\perp = 3$, provided that the diffusion length in the z direction is within the confining wall. As a result, we have the Bekenstein-Hawking-type relation,

$$\frac{\mathbf{S}_{\rm BH}}{A_{\rm BH}} \equiv \frac{1}{4G_5}, \tag{69}$$

with an effective Newton constant,

$$G_5 = \pi^2((\chi/k^3)(1-\tilde{\beta}_H^2/\beta^2))^{1/2} l_s^3. \tag{70}$$

For a fundamental string, the Planck and string constants are related with G_5 through $G_5 = l_P^3 = g_s^2 l_s^3$. We recall that in the large N_c counting $g_s^2 \approx 1/N_c^2$.

The transmutation of the near-critical strings into a black-hole at the string scale was foreseen by Susskind and others in the context of string-based gravity [54,55]. Furthermore, it was later shown that the Bekenstein-Hawking formulas emerge from a direct statistical counting of quantum string states. In hadronic collisions at large rapidity χ, the effective relation (70) shows that this transmutation can be achieved in a twofold way: (i) one is discussed in this paper, $\beta/\tilde{\beta}_H \to 1$ (the near-critical regime), and the other (ii) is a more exotic case possible in the large N_c limit, namely the exchange of a string with very large color charge $k/\chi \to \infty$ which we do not discuss.

Empirical estimates based on DIS data analysis [2] suggest that the saturation scale is $z_0 \approx 2/\text{GeV}$, so that the diffusion length is far from the confining wall for $\sqrt{\chi/k} l_s < z_0$ or $\chi < 16$ for $k = 1$. For very high energy collisions, however, given by $\chi > 16$ the diffusion length reaches the confining wall. This should modify scattering at superhigh energies; in particular, the transverse area (68) is now changed to

$$A_{\rm BH} \approx 2\pi^2 z_0 (\sqrt{\chi/k} l_s)^2, \tag{71}$$

with the corresponding changes in the effective Newton constant estimate,

$$G_5 = (\pi^2/k)(1-\tilde{\beta}_H^2/\beta^2)^{1/2}(z_0 l_s^2). \tag{72}$$

A. Dual derivation of the string propagators

We can explicitly check that the tachyon thermodynamics (64) and (66) follows from the large n excitation spectrum of the NG string by using the modular transformation and the saddle point approximation in flat space. The modular transform of the transverse string propagator is an exchange $b \leftrightarrow \beta$, which corresponds to going into the close string description from the open strings. It is basically a change of coordinates in string quantization, describing the same "tube" configuration. Indeed, the modular transform of (22) can be cast as

$$\mathbf{K}_T(\beta, \mathbf{b}; k) \approx \sum_{n=0}^{\infty} d(n) e^{-\sigma\beta\mathbf{b}(1-\mathbf{b}_c^2/\mathbf{b}^2+2\pi n/\sigma\mathbf{b}^2)^{1/2}}, \tag{73}$$

with $\mathbf{b}_c = ((\pi D_\perp)/(12\sigma))^{1/2} \equiv \pi l_s$ and the density of states (A2). The NG form has been subsumed. Equation (73) is seen to diverge for $\beta \le \beta_H$. The divergence is controlled by a large n saddle point,

$$n_S \approx \frac{\sigma\mathbf{b}^2}{2\pi} \frac{1}{(\beta/\beta_H)^2 - 1} \gg 1, \tag{74}$$

for which (73) is to exponential accuracy,

$$\mathbf{K}_T(\beta, \mathbf{b}; k) \approx e^{-\sigma\mathbf{b}\sqrt{\beta^2-\beta_H^2}}, \tag{75}$$

in agreement with the tachyon result above.

The string energy at the large n saddle point (74) is

$$\mathbf{E} \approx \sigma\mathbf{b}\sqrt{\frac{2\pi n_S}{\sigma\mathbf{b}^2}} = \frac{\sigma\mathbf{b}}{\sqrt{\beta^2/\beta_H^2 - 1}}, \tag{76}$$

and the corresponding entropy is

$$\mathbf{S} \equiv \ln d(n_S) = 2\pi\sqrt{\frac{D_\perp n_S}{6}} - \frac{D_\perp}{4}\ln n_S, \tag{77}$$

which is seen to satisfy the zero pressure condition $\mathbf{S} \approx \beta_H \mathbf{E}$ in leading order. They are the tachyonic energy and entropy in the Hagedorn limit discussed above. This is expected since the modular transform allows us to cross from the $\beta < \mathbf{b}$ regime of long and close strings, to the $\beta > \mathbf{b}$ of short and open strings. The two descriptions match at the border $\mathbf{b} \approx \beta$.

At the Hagedorn limit, a long and space filling string, with $D_\perp$ dimensions, is a very efficient way to carry large entropy. The analogy between a string ball and black hole thermodynamics shows that in fact it carries the largest entropy density possible. With this in mind and for simplicity, consider a Polyakov string made of $D_\perp$ harmonic oscillators immersed in a heat bath with finite but large Rindler temperature $1/\beta_R$. The energy of the string is dominated by the high-frequency modes,

$$\mathbf{E}_R \approx D_\perp \sum_{n=1}^{\infty} \frac{n}{e^{\beta_R n} - 1}. \tag{78}$$

For large $1/\beta_R$ it is the black body,

$$\mathbf{E}_R \approx \frac{\pi^2}{2\beta_R^2} \frac{D_\perp}{3}. \tag{79}$$

Through the first law of thermodynamics (66) we can enforce the zero pressure condition on this highly excited string, with

$$\mathbf{S} \equiv \mathbf{S}_R \approx \beta_R \mathbf{E}_R = \frac{\pi^2}{2\beta_R}\frac{D_\perp}{3}. \tag{80}$$

B. Viscosity at the Rindler horizon

Viscosity can be defined via certain limits of the correlators of the stress tensor, known as the Kubo formula. Thus one does not need hydrodynamics to calculate it, just the stress tensor. To assess the primordial viscosity, we follow [3] and write the needed expression on the stretched horizon for the excited string,

$$\eta_R = \lim_{\omega_R \to 0} \frac{A_R}{2\omega_R} \int_0^\infty d\tau e^{i\omega_R \tau} \mathbf{R}_{23,23}(\tau), \tag{81}$$

with A_R the area of the black hole and τ a dimensionless Rindler time. The retarded commutator of the normal ordered transverse stress tensor for the Polyakov string on the Rindler horizon reads

$$\mathbf{R}_{23,23}(\tau) = \langle [T_\perp^{23}(\tau), T_\perp^{23}(0)] \rangle, \tag{82}$$

with

$$T_\perp^{23}(\tau) = \frac{1}{2A_R} \sum_{n \neq 0} : a_n^2 a_n^3 : e^{-2in\tau}, \tag{83}$$

and the canonical rules $[a_m^i, a_n^j] = m\delta_{m+n,0}\delta^{ij}$. The averaging in (82) is carried using the black-body spectrum as in (78). The result is

$$\eta_R = \lim_{\omega_R \to 0} \frac{A_R}{2\omega_R} \frac{\pi}{2A_R^2} \frac{(\omega_R/2)^2}{e^{\beta_R \omega_R/2} - 1} = \frac{1}{A_R}\frac{\pi}{8\beta_R}. \tag{84}$$

We note the occurrence of the Bekenstein-Hawking or Rindler temperature $\beta_{\rm BH} = \beta_R$ in the thermal factor.

Combining (80) for the entropy to (84) yields the viscosity on the stretched horizon,

$$\frac{\eta_R}{\mathbf{S}_\mathbf{R}/A_R} = \frac{1}{4\pi}\left(\frac{3}{D_\perp}\right) \equiv \frac{1}{4\pi}, \tag{85}$$

which, for $D_\perp = 3$, is precisely the celebrated universal value from AdS/CFT. The result (85) is remarkable as it follows solely from a string moving at large "time" χ in noncritical dimensions but near its Rindler horizon, not in transverse coordinate z. It emerges naturally in the near-Hagedorn regime.

The result (85) for the critical Pomeron as a close string exchange on the stretched horizon for large $1/\beta_R$ is to be contrasted to the same viscosity ratio but for the low-T Pomeron as a close string exchange far from the horizon for small $1/\beta_k$ [3],

$$\frac{\eta_\perp}{\mathbf{S}/A_\perp} = \frac{1}{2}\frac{1}{4\pi}\left(\frac{2\pi}{\beta_k}\right)^2\left(\frac{3}{D_\perp}\right). \tag{86}$$

The ratio is small at large rapidity. Equation (86) reduces to (85) for $\beta_k \to \beta_R$ up to a factor of $1/2$, showing the noncommutativity of the two limits. Indeed, for small $1/\beta_k$ the noncritical Pomeron is described by the Polyakov action whereby the zero pressure condition (emblematic of a near-Hagedorn or black hole in Rindler coordinates) does not hold.

Furthermore, the relation (84) yields an effective viscosity for finite frequency (but still zero momentum) to be thermally suppressed for the large frequency modes ω_R,

$$\eta_R(\omega_R) = \frac{\pi}{16A_R}\frac{\omega_R}{e^{\omega_R/2T_R} - 1}. \tag{87}$$

The onset of the black hole is followed by Hawking radiation of string bits of frequency $\omega_R/2$ as is explicit in (87) and stressed further below. In particular, for finite wave number k_R in Rindler units, the suppression is physically expected to follow from the substitution

$$\omega_R \to \sqrt{\omega_R^2 + k_R^2}, \tag{88}$$

and therefore from the exponential as well. The effective viscosity $\eta_R(\omega_R, k_R)$ at higher gradients—larger k_R—would indeed imply a smaller effective viscosity in pp than in AA. This point is similar to the Lublinsky-Shuryak re-summation scheme [56].

Concluding this discussion of the viscosity let us make the following comment. While one can use the Kubo formula for any setting in which the stress tensor is defined, the resulting viscosity itself is of hardly any use outside of hydrodynamics. As we emphasized above, phenomenology indicates that in an "explosive" regime with very high multiplicity there are hydrodynamical flows. Alas, both for the cool subcritical strings and the near-critical strings, flows are absent. The results of this subsection can only be used for the near-critical regime. Specifically, they can either be used to account for nonhydro dissipative phenomena, or perhaps even for the viscosity at the late stages of the explosive process, as the system returns to the near-critical regime.

C. Hawking radiation

In a typical pp and pA collision in the "cold" regime, a pair of strings is created in the scattering process and then stretched longitudinally to finally decay via the Schwinger pair-production mechanism. The decay process is captured by the Lund model in event generators. The production of the final—observables—entropy and temperature in the "near-critical" regime are related to its black-hole-based description. Standard particle emission from a black hole is described as the Hawking radiation.

We ascribed to high-multiplicity events a somewhat different particle emission mechanism. This emission is fully thermal. However, it does not require long equilibration time of the fireball, and it takes place because the near-horizon zero point oscillations of quantum fields apparently appear in a thermal form. One may call it "prompt thermal emission," not delayed by the usual equilibration processes. At this point our approach is similar in spirit but different in details to the Unruh-Hawking effect discussed in [57].

The power spectrum or Hawking emission per unit time from a black hole is generic. For our rapidly moving string it involves a black-hole in $1+4$ dimensions with the extra dimension accounting for changes in the dipole scales. In $D_\perp+2$ dimensions it reads [58]

$$d^{D_\perp+1}\mathbf{P}=\sum_s \sigma_s(\omega)\frac{\omega}{e^{\omega/T_{\rm BH}}+(-1)^{2s+1}}\frac{d^{D_\perp+1}k}{(2\pi)^{D_\perp+1}}. \quad (89)$$

We have only kept the dominant S-wave contributions. Here $T_{\rm BH}=T_R=1/(2\pi l_s)$. The sum runs over the spin s of the emitted particle with $\sigma_s(\omega)$ the S-wave absorption cross section or grey-body factor of a spin-s on a black hole. For $\omega l_s\ll 1$,

$$\sigma_s(\omega)\approx\kappa_s A_{\rm BH}\equiv 4\kappa_s l_P^{D_\perp+1}\mathbf{S}, \quad (90)$$

with $A_{\rm BH}$ the area of the black hole. The last identity follows from the Bekenstein-Hawking type relation and shows that the power spectrum is extensive with the entropy. For scalars $\kappa_s=1$ [58]. As the Hawking emission through (90) unfolds, the mass and radius of the black hole decreases, causing the Hawking temperature $T_{\rm BH}$ to increase. The emission process is inherently a nonequilibrium one. Here and for simplicity, we assume it to be quasiadiabatic with (90) adjusting to the change in $T_{\rm BH}$.

For massless particles, $\omega=|k|$ in (90). The luminosity defined as $\mathbf{L}(\omega)=d\mathbf{P}/d\omega$ for $D_\perp=3$ is

$$\mathbf{L}(\omega)=\frac{A_{\rm BH}}{8\pi^2}\sum_s \kappa_s\frac{\omega^4}{e^{\omega/T_{\rm BH}}+(-1)^{2s+1}}. \quad (91)$$

It is a black-body spectrum from a five-dimensional space where the black hole originated.

As many of these black holes are expected to be released in AA collisions, they are the seeds of the primordial matter viewed as a collection of these tiny black holes. Primordial Hawking emission of partonic constituents as well as electromagnetic radiation is what current heavy ion colliders are probing. We recall that for $\chi<16$ we have $A_{\rm BH}\approx\chi^{3/2}$, while for $\chi>16$ we have $A_{\rm BH}\approx\chi$ because of confinement in the holographic or conformal direction of the string. Therefore, we estimate the thresholds $\mathbf{N}_T(\chi)$ for the large multiplicity events with explosive hydrodynamical flow to scale with beam rapidity as

$$\frac{\mathbf{N}_T(\chi_1)}{\mathbf{N}_T(\chi_2)}=\left(\frac{\chi_1}{\chi_2}\right)^{3/2} \quad (92)$$

for $\chi_{1,2}<16$ and 1 for $\chi_{1,2}>16$, irrespective of whether they are pp, pA or AA collisions.

VIII. DISCUSSION

A. Summary

We have started by a review of the SZ Pomeron model, based on an exchange of a noncritical string in curved AdS_5-like space with a confining wall. For typical collision events at current energies, including the LHC domain, the Pomeron follows from the string quantized via the scalar Polyakov action for the slightly excited string oscillators. A relatively small Luscher term generates the intercept of the Pomeron (23), which for $D_\perp=3$ and, with a finite $1/\lambda$ correction, yields a value acceptably close to the phenomenological soft Pomeron intercept. The slope and the "daughter" trajectories are also found to be at the phenomenologically appropriate places.

In this paper, we further discussed fluctuations of the virtual strings, describing those by an effective temperature. For typical min-bias collisions we found $T_{\rm eff}$ to be sufficiently far from the Hagedorn temperature $\tilde{T}_H$, to justify the use of the "cold" regime for the SZ Pomeron and its excitations. (Recall that the tilde is a reminder of the upward shift in the temperature caused by the AdS_5 curvature).

The essential part of our work is about either higher-than-LHC collision energy or central collisions with an impact parameter $\mathbf{b}$ less than typical. These collisions have higher $T_{\rm eff}$ which approaches $\tilde{T}_H$ the Hagedorn temperature. We argued that in this case the string enters a new near-critical regime, in which one expects the proliferation of long strings in the form of a self-interacting string ball. Such a phenomenon at the corresponding temperature in a truly thermodynamical setting is well known, but we argued that it should also happen without a heat bath, with an individual string created in the collisions.

We further argued that as the mass density of the string ball reaches a sufficiently high value, the string ball becomes a black hole. At still lower impact parameter the transition to the third—postcritical or explosive—regime takes place, in which the system becomes amenable to a macroscopic—hydrodynamical—description. It is in this regime that strong radial, elliptic (the so-called "ridge") and even triangular flows have been detected. We argued that the second regime would get dominant at the energies corresponding to the highest end of the LHC energy domain.

While these phenomena do not (yet) correspond to the typical (min-bias) collisions at existing experimental conditions, being still in the "cold string" regime and

amenable to the SZ Pomeron description developed earlier, a certain fraction of the more central events should display the newly suggested regimes. We argued that the high-multiplicity pp and pA events, triggered experimentally by certain criteria, are dominated by such regimes. In particular, we suggested that the production of a string-ball cluster in the middle of the string (midrapidity) is the reason for this multiplicity.

The theoretical description of the new regimes is as follows. When the effective temperature approaches the Hagedorn temperature, string excitations are no longer small, and the expression for the string propagator (22) is to be reconsidered. We do so by using the known results for the resummed confining potential with all-order Luscher terms for the Nambu-Goto string action, resulting in the new expression (48). For such a string its tension effectively vanishes, leading to a string-ball formation.

All properties of a sufficiently massive string ball are shown to reach those of a black hole. The particle production from such a string ball follows Hawking thermal radiation pattern. Unlike most holographic models, this black hole does not have a horizon along the z direction. It is produced in the collision and its Rindler horizon is along the longitudinal direction. This black hole is five dimensional, with three transverse coordinates, two spatial ones and one conformal z describing the scale evolution. The black-hole radius and area are set by the Gribov diffusion length, which grows with the collision energy $\chi = \ln(s/s_0)$ as $\chi^{1/2}$, and $\chi^{3/2}$ for $\chi < 16$, respectively. For very high collision energies $\chi > 16$, the area growth is reduced to χ because of confinement along the holographic or conformal direction of the string.

We have thus argued that for sufficiently central collisions the final state should contain remnants of the string hole. While we have not discussed in this paper its evolution after $t = 0$ (the moment when strings appear from under-the-barrier), let us add at least two comments. These remnants should be seen as clusters visible in two- (or more)-body rapidity correlations. Furthermore, as evident from Fig. 2, pulling the strings along two arrows longitudinally would provide the cluster an angular momentum. Its magnitude would only be limited by the string breaking. This means that the produced clusters should have angular momentum $\vec{J}$, that maybe significant and normal to the scattering plane. This momentum would generate certain angular correlations in the transverse plane.

Using the Kubo formula for string excitations, we found that on the stretched or Rindler horizon the shear viscosity to entropy ratio is precisely $1/4\pi$, for $D_\perp = 3$. It is the same as for the AdS/CFT black hole, in spite of the fact that these two black holes are very different. Ours is dynamical with a horizon normal to the longitudinal coordinate, while the AdS/CFT one is static, with a horizon normal to the transverse holographic z direction.

We have further argued that when the temperature exceeds the Hagedorn value, one approaches the postcritical regime. Its most adequate description is generation of a black hole. Its Hawking radiation is seen as a QGP fireball. As a result, the transition to the deconfined phase unleashes a large pressure with $p \approx \epsilon/3$ and the stringy black hole explodes hydrodynamically, following the general scaling of viscous hydrodynamics in small volumes. The macroscopic treatment of these effects is discussed elsewhere [6].

ACKNOWLEDGMENTS

We would like to thank Alex Stoffers, Gokce Basar, Dima Kharzeev and Derek Teaney for discussions. This work was supported in part by the U.S. Department of Energy under Contract No. DE-FG-88ER40388.

APPENDIX: ON THE DENISTY OF STATES

There are many definitions for the string density of states. As noted in [22], in mathematics it goes back at least to 1918 in the famed Hardy-Ramanujan paper. One definition consists in expanding the string of products,

$$\prod_{k=1}^{\infty}\left(\frac{1}{1-\xi^k}\right)^{D_\perp} = \sum_{n=0}^{\infty} d(n)\xi^n. \tag{A1}$$

For our case, $D_\perp = 3$ and the first coefficients are 1, 3, 9... as easily obtained by an expansion in series.

The asymptotic density of states is known, see e.g. [59], as

$$d(n \gg 1) \approx C e^{2\pi\sqrt{D_\perp n/6}}/n^{D_\perp/4}, \tag{A2}$$

where C is a constant. We have checked the validity of this formula for the first dozen terms, see Fig. 15. We have chosen to normalize exactly the tenth term, using $C = 0.01174701111$.

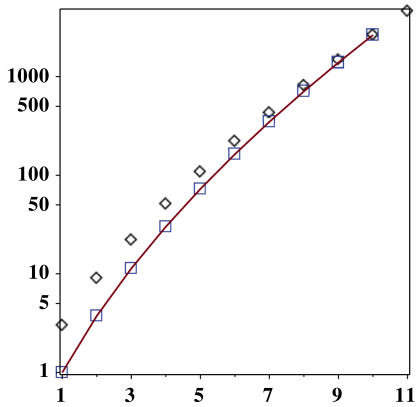

FIG. 15 (color online). The density of states $d(n)$ versus n. Black diamonds show the exact result, while the squares and the curve correspond to the asymptotic expression (A2).

[1] A. Stoffers and I. Zahed, Phys. Rev. D **87**, 075023 (2013).
[2] A. Stoffers and I. Zahed, Phys. Rev. D **88**, 025038 (2013).
[3] I. Zahed, arXiv:1211.6421.
[4] A. Stoffers and I. Zahed, arXiv:1210.3724; Acta Phys. Pol. B Proc. Suppl. **6**, 7 (2013).
[5] G. Basar, D. E. Kharzeev, H. U. Yee, and I. Zahed, Phys. Rev. D **85**, 105005 (2012).
[6] E. Shuryak and I. Zahed, Phys. Rev. C **88**, 044915 (2013).
[7] E. A. Kuraev, L. N. Lipatov, and V. S. Fadin, Sov. Phys. JETP **45**, 199 (1978); Ya. Ya. Balitsky and L. N. Lipatov, Sov. J. Nucl. Phys. **28**, 22 (1978).
[8] M. Rho, S. -J. Sin, and I. Zahed, Phys. Lett. B **466**, 199 (1999).
[9] R. A. Janik, Phys. Lett. B **500**, 118 (2001); R. A. Janik and R. B. Peschanski, Nucl. Phys. **B586**, 163 (2000).
[10] R. A. Janik and R. B. Peschanski, Nucl. Phys. **B625**, 279 (2002).
[11] J. Polchinski and M. J. Strassler, J. High Energy Phys. 05 (2003) 012; J. Polchinski and M. J. Strassler, Phys. Rev. Lett. **88**, 031601 (2002); R. C. Brower, J. Polchinski, M. J. Strassler, and C. I. Tan, J. High Energy Phys. 12 (2007) 005; R. C. Brower, M. J. Strassler, and C.-ITan, J. High Energy Phys. 03 (2009) 092; R. C. Brower, M. Djuric, and C.-ITan, J. High Energy Phys. 07 (2009) 063; R. C. Brower, M. Djuric, and C.-ITan, arXiv:0812.1299; R. C. Brower, M. Djuric, I. Sarcevic, and C. -ITan, J. High Energy Phys. 11 (2010) 051; R. C. Brower, M. Djuric, I. Sarcevic, and C. -ITan, arXiv:1106.5681; M. S. Costa and M. Djuric, AIP Conf. Proc. **1523**, 91 (2012); M. S. Costa, M. Djuric, and N. Evans, J. High Energy Phys. 09 (2013) 084.
[12] L. Cornalba, M. S. Costa, and J. Penedones, Phys. Rev. Lett. **105**, 072003 (2010); L. Cornalba, M. S. Costa, J. Penedones, and P. Vieira, J. High Energy Phys. 12 (2006) 023.
[13] Y. Hatta, E. Iancu, and A. H. Mueller, J. High Energy Phys. 01 (2008) 063; Y. Hatta, E. Iancu, and A. H. Mueller, J. High Energy Phys. 01 (2008) 026.
[14] J. L. Albacete, Y. V. Kovchegov, and A. Taliotis, J. High Energy Phys. 07 (2008) 074; J. L. Albacete, Y. V. Kovchegov, and A. Taliotis, AIP Conf. Proc. **1105**, 356 (2009).
[15] V. Khachatryan (CMS Collaboration), J. High Energy Phys. 09 (2010) 091.
[16] S. Chatrchyan (CMS Collaboration), Phys. Lett. B **718**, 795 (2013).
[17] B. Abelev *et al.* (ALICE Collaboration), Phys. Lett. B **719**, 29 (2013).
[18] G. Aad *et al.* (ATLAS Collaboration), Phys. Rev. Lett. **110**, 182302 (2013).
[19] A. Adare *et al.* (PHENIX Collaboration), Phys. Rev. Lett. **111**, 212301 (2013).
[20] R. Hagedorn, Nuovo Cimento Suppl. **3**, 147 (1965).
[21] S. Fubini and G. Veneziano, Nuovo Cimento A **64**, 811 (1969).
[22] K. Huang and S. Weinberg, Phys. Rev. Lett. **25**, 895 (1970).
[23] A. M. Polyakov, Phys. Lett. **82B**, 247 (1979).
[24] L. Susskind, Phys. Rev. D **20**, 2610 (1979).
[25] S. Lin and E. Shuryak, Phys. Rev. D **79**, 124015 (2009).
[26] S. S. Gubser, S. S. Pufu, and A. Yarom, J. High Energy Phys. 11 (2009) 050.
[27] V. N. Gribov and I. Y. .Pomeranchuk, Zh. Eksp. Teor. Fiz. **42**, 1141 (1962); Sov. Phys. JETP **15**, 788L (1962); Phys. Rev. Lett. **8**, 343 (1962).
[28] V. N. Gribov, Zh. Eksp. Teor. Fiz. **53**, 654 (1967); Sov. Phys. JETP **26**, 414 (1968).
[29] V. A. Abramovsky, V. N. Gribov, and O. V. Kancheli, Sov. J. Nucl. Phys. **18**, 308 (1974); Yad. Fiz. **18**, 595 (1973).
[30] E. Levin, J. High Energy Phys. 11 (2013) 039.
[31] G. Veneziano, Nuovo Cimento A **57**, 190 (1968).
[32] J. Greensite, Nucl. Phys. **B249**, 263 (1985).
[33] J. M. Maldacena, Phys. Rev. Lett. **80**, 4859 (1998).
[34] G. Antchev *et al.* (TOTEM Collaboration), Europhys. Lett. **95**, 41001 (2011).
[35] C. Bourrely, J. M. Myers, J. Soffer, and T. T. Wu, Phys. Rev. D **85**, 096009 (2012).
[36] In this model as $\exp(-m_1\mathbf{b})$, $m_1 = 0.577$ GeV, perhaps representing σ exchange.
[37] C. J. Morningstar and M. J. Peardon, Phys. Rev. D **60**, 034509 (1999).
[38] Harvey B. Meyer, arXiv:hep-lat/0508002.
[39] M. Teper, Acta Phys. Pol. B **40**, 3249 (2009).
[40] J. F. Arvis, Phys. Lett. B **127**, 106 (1983).
[41] B. Bringoltz and M. Teper, Phys. Rev. D **73**, 014517 (2006).
[42] F. Sauter, Z. Phys. **69**, 742 (1931).
[43] A. H. Mueller, Nucl. Phys. **B415**, 373 (1994).
[44] A. H. Mueller and B. Patel, Nucl. Phys. **B425**, 471 (1994).
[45] G. P. Salam, Nucl. Phys. **B461**, 512 (1996).
[46] For definiteness, we use the PDG parametrization $\sigma_{\mathbf{P}}(s) = 35.45 + 0.308 * \ln^2(0.1381 * \gamma^2)$ with $s = 4M^2\gamma^2$.
[47] I. A. Kogan, JETP Lett. **45**, 709 (1987); J. J. Attick and E. Witten, Nucl. Phys. **B310**, 291 (1988).
[48] G. T. Horowitz and J. Polchinski, Phys. Rev. D **57**, 2557 (1998).
[49] T. Damour and G. Veneziano, Nucl. Phys. **B568**, 93 (2000).
[50] T. Kalaydzhyan and E. Shuryak, arXiv:1402.7363.
[51] A. H. Mueller, Phys. Rev. D **2**, 2963 (1970); O. V. Kancheli, JETP Lett. **11**, 267 (1970).
[52] D. Velicanu (CMS Collaboration), J. Phys. G **38**, 124051 (2011).
[53] K. Dusling and R. Venugopalan, Phys. Rev. D **87**, 054014 (2013); Phys. Rev. D **87**, 051502 (2013); Phys. Rev. Lett. **108**, 262001 (2012).
[54] L. Susskind, in *The Black Hole*, edited by C. Teitelboim (World Scientific, Singapore, 1998), p. 118; L. Susskind, Phys. Rev. D **49**, 6606 (1994).
[55] A. Strominger and C. Vafa, Phys. Lett. B **379**, 99 (1996); R. R. Khuri, Nucl. Phys. **B588**, 253 (2000).
[56] M. Lublinsky and E. Shuryak, Phys. Rev. D **80**, 065026 (2009).
[57] D. Kharzeev, Eur. Phys. J. A **29**, 83 (2006); P. Castorina, D. Kharzeev, and H. Satz, Eur. Phys. J. C **52**, 187 (2007).
[58] S. R. Das, G. W. Gibbons, and S. D. Mathur, Phys. Rev. Lett. **78**, 417 (1997).
[59] S. Fubini, D. Gordon, and G. Veneziano, Phys. Lett. **29B**, 679 (1969).